

## Article

# Genome-Wide Identification and Expression Analysis of the Zinc Finger Protein Gene Subfamilies under Drought Stress in *Triticum aestivum*

Zhaoming Wu<sup>1</sup>, Shenghai Shen<sup>1</sup> , Yueduo Wang<sup>1</sup>, Weiqi Tao<sup>2</sup>, Ziqi Zhao<sup>1</sup>, Xiangli Hu<sup>1</sup> and Pei Yu<sup>1,2,3,\*</sup><sup>1</sup> SDU-ANU Joint Science College, Shandong University, Weihai 264209, China<sup>2</sup> Marine College, Shandong University, Weihai 264209, China<sup>3</sup> Research Center for Biological Adaptability in Space Environment, Institute of Space Sciences, Shandong University, Weihai 264209, China

\* Correspondence: yupei@sdu.edu.cn

**Abstract:** The zinc finger protein (ZFP) family is one of plants' most diverse family of transcription factors. These proteins with finger-like structural domains have been shown to play a critical role in plant responses to abiotic stresses such as drought. This study aimed to systematically characterize *Triticum aestivum* ZFPs (TaZFPs) and understand their roles under drought stress. A total of 9 TaC2H2, 38 TaC3HC4, 79 TaCCCH, and 143 TaPHD were identified, which were divided into 4, 7, 12, and 14 distinct subgroups based on their phylogenetic relationships, respectively. Segmental duplication dominated the evolution of four subfamilies and made important contributions to the large-scale amplification of gene families. Syntenic relationships, gene duplications, and Ka/Ks result consistently indicate a potential strong purifying selection on TaZFPs. Additionally, TaZFPs have various abiotic stress-associated *cis*-acting regulatory elements and have tissue-specific expression patterns showing different responses to drought and heat stress. Therefore, these genes may play multiple functions in plant growth and stress resistance responses. This is the first comprehensive genome-wide analysis of ZFP gene families in *T. aestivum* to elucidate the basis of their function and resistance mechanisms, providing a reference for precise manipulation of genetic engineering for drought resistance in *T. aestivum*.

**Keywords:** genome-wide identification; abiotic stresses; zinc finger proteins; expression pattern; drought stress; *Triticum aestivum*



**Citation:** Wu, Z.; Shen, S.; Wang, Y.; Tao, W.; Zhao, Z.; Hu, X.; Yu, P. Genome-Wide Identification and Expression Analysis of the Zinc Finger Protein Gene Subfamilies under Drought Stress in *Triticum aestivum*. *Plants* **2022**, *11*, 2511. <https://doi.org/10.3390/plants11192511>

Academic Editor: Daniela Trono

Received: 29 July 2022

Accepted: 22 September 2022

Published: 26 September 2022

**Publisher's Note:** MDPI stays neutral with regard to jurisdictional claims in published maps and institutional affiliations.



**Copyright:** © 2022 by the authors. Licensee MDPI, Basel, Switzerland. This article is an open access article distributed under the terms and conditions of the Creative Commons Attribution (CC BY) license (<https://creativecommons.org/licenses/by/4.0/>).

## 1. Introduction

Plants may experience a variety of complex environmental stresses during their lifetime. With environmental problems such as greenhouse gases and soil pollution, abiotic stresses are becoming more common [1]. Stresses such as drought, heat, and high salinity can limit the growth and yield of crops. This phenomenon has profound implications for agriculture, forestry, and global food security issues. However, plants have evolved multiple regulatory pathways involving many transcription factor families to receive and respond to different stress signals [2,3]. Various protein families are able to regulate plant physiological processes by modifying gene expression, altering signalling, and interfering with biosynthesis to improve their adaptability [4–7].

The large and diverse zinc finger protein (ZFP) family plays a crucial role in various aspects of plant growth and development. ZFP has a highly conserved structural domain of about 30 amino acids [8,9]. As an essential motif, ZFP is involved in several physiological processes such as specific binding of proteins to DNA/RNA, protein-protein interactions, and membrane association [10]. The plant genome encodes a large number of ZFPs, the most representative being the C2H2-type, C3HC4-type, CCCH-type, and PHD-type. In addition to its role in seed germination and organ development, many studies have shown

that ZFP is closely related to plants' physiological and metabolic processes of various abiotic stress responses [11–13]. These protein factors are activated by stress and then alter plant tolerance through complex networks and molecular mechanisms. For instance, gene expression and crosstalk with phytohormones are directly regulated through the ABA-mediated and the mitogen-activated protein kinase (MAPK) signalling pathway [11]. For example, ZFP CCCH in *Arabidopsis thaliana* enhance survival by increasing the expression levels of osmoregulatory substances with enhanced expression of related stress genes [14]. The C2H2-type proteins ZFP245 and ZFP179 in *Oryza sativa* promoted the amount of free proline and soluble sugars, elevated the expression of stress-responsive genes, and enhanced their tolerance to salt and drought stresses [15]. Under cold environments, ZFP C2H2 directly regulates downstream genes to enhance cold resistance in *Sorghum bicolor* [16]. Additionally, ZFP in *Glycine soja* enhances salt tolerance by maintaining ion homeostasis and removing peroxides [17]. In summary, ZFPs play important roles in plant development and abiotic stress resistance, and in-depth studies of these proteins are necessary to understand their functions and mechanisms better.

Due to the extensive interest in their positions in the physiological regulation of resistance, some ZFP families have been identified and investigated in various plants, such as *A. thaliana*, *Solanum tuberosum*, *Pleurotus ostreatus*, and *Cucumis sativus* [18–22]. However, this functionally diverse family of proteins has not been studied in wheat (*Triticum aestivum*). *T. aestivum* is one of the most widely grown cereals in the world and is extensively used for industrial production [23]. It is the main ingredient in many marketed animal feeds, brewed beverages, and processed foods. The demand for *T. aestivum* as part of the global population's diet is expected to reach over 900 million tonnes in 2050 [24]. As a result, *T. aestivum* exhibits outstanding economic and industrial value. *T. aestivum*'s breeding, cultivation, and responsiveness to the environment have been a hot research topic in plant science and agronomy. Abiotic stresses such as drought are often considered significant in limiting *T. aestivum* growth [25]. Therefore, it is necessary to study the characteristics of transcription factors that respond to abiotic stresses and thus improve the understanding of *T. aestivum* stress tolerance mechanisms. Several ZFP functions in *T. aestivum* have been reported and demonstrated for their responsiveness to abiotic stresses. However, a systematic genome-wide analysis targeting four subfamilies has not yet been performed. This is crucial for a comprehensive study of the characterization and physiological aspects of the TaZFP genes. In this study, we performed a genome-wide identification of 269 *T. aestivum* ZFPs (TaZFPs) and analyzed their phylogenetic relationships, structural features, physicochemical properties, and interactions networks. In addition, the expression pattern of the specific TaZFPs under drought stress was investigated using publicly available expression profiles and quantitative real-time PCR (qRT-PCR). Overall, this study provides insight into the characterization and structure of TaZFPs, lays the foundation for illustrating its biological function in response to abiotic stress, and provides theoretical support for further genetic engineering design.

## 2. Results

### 2.1. Identification and Chromosomal Distribution of the TaZFPs

Based on HMM searches of the core structural domains of the four subfamilies of TaZFPs (C2H2: PF00096, C3HC4: PF00097, CCCH: PF00642, and PHD: PF00628) and sequence alignment of ZFP gene subfamilies from *A. thaliana*, a total of 269 non-redundant TaZFPs were identified, which contained 9 TaC2H2, 38 TaC3HC4, 79 TaCCCH, and 143 TaPHD.

The predicted physicochemical properties of TaZFPs (Table S1) showed that, except for two sequences with a large number of unknown amino acids that could not be calculated, the length of TaZFPs ranged from 148 to 2092 aa, and the molecular weight ranged from 16.22 to 231.86 kDa. The isoelectric point of TaZFPs ranged from 4.42 to 9.85, indicating that TaZFPs contain both acidic and basic protein types. The instability index of TaZFPs varied from 35.82 to 84.75, of which only 13 protein sequences were considered stable. The

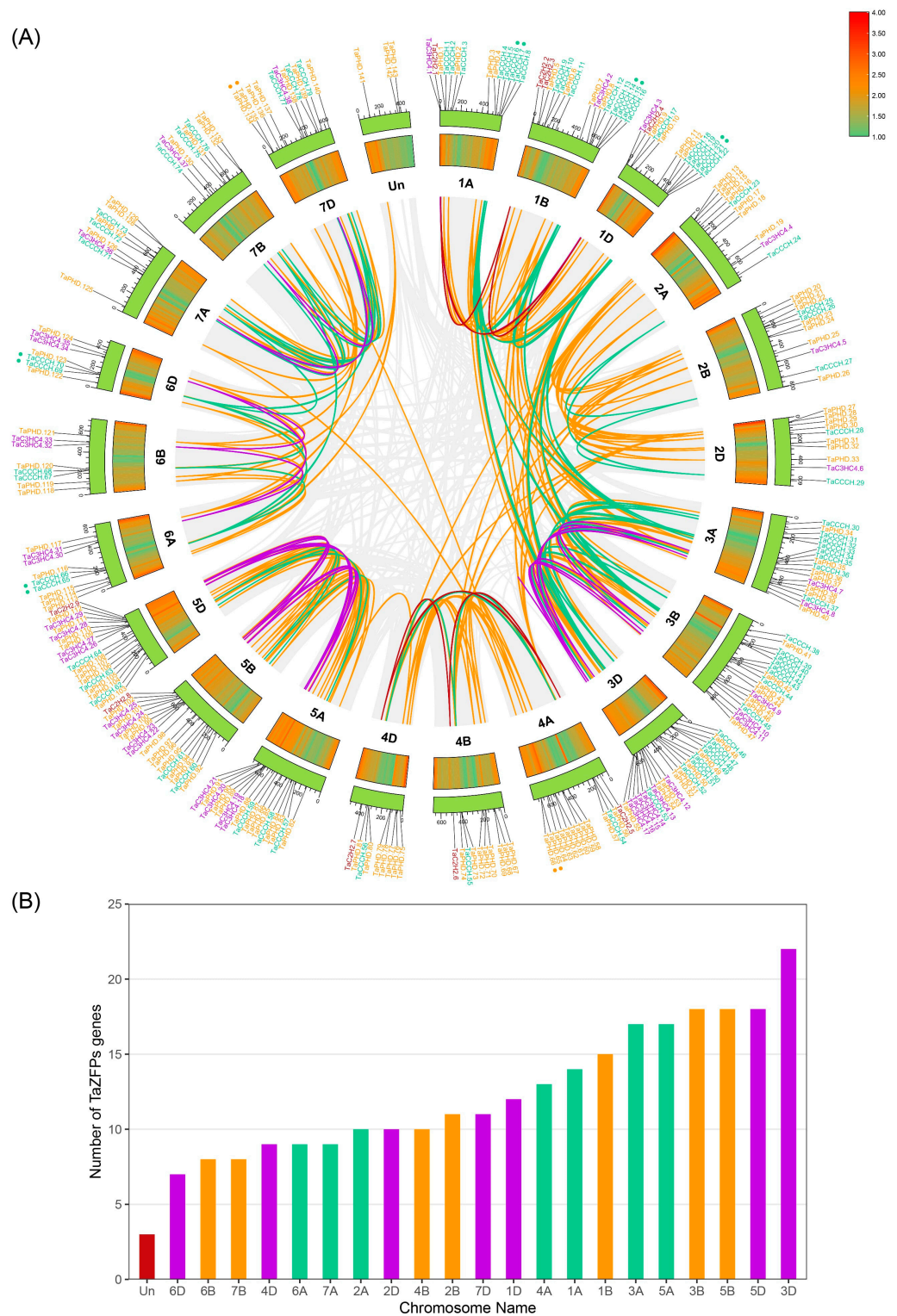
aliphatic index of TaZFPs ranged from 39.08 to 102.28, and its globular protein thermal stability has diverse characteristics. According to the hydrophilicity index, 98.89% of TaZFPs are hydrophilic, with TaCCCH.76 being the strongest ( $-1.404$ ) and TaPHD.108 being the weakest ( $-0.004$ ). Generally, there is a diversity of physicochemical properties such as length, relative molecular mass, isoelectric point, and hydrophilicity index between the different ZFPs.

TBtools was used to create a chromosome map of the TaZFPs based on the physical location information provided by the *T. aestivum* gff3 file. TaZFPs were present on all 21 *T. aestivum* chromosomes and were unevenly distributed (Figure 1), whereas three TaPHD genes could not be localized to any chromosome. The specific distribution of TaZFPs on the chromosomes is detailed in Table S1. Meanwhile, TaZFP genes were equally distributed on *T. aestivum* subgenomes A, B, and D, with localization numbers of 88, 88, and 89, respectively. Chromosome 3 had the highest density of TaZFPs, with 57 on chromosome 3D and 17 and 18 on each of chromosome 3A and 3B, respectively. Chromosome 6D had the lowest number of TaZFPs, with only seven. Among the TaCCCH gene subfamilies, chromosomes 1A and 3D had the highest densities. Moreover, group 4 homologs had the lowest density and number of homologs, with almost equal numbers in the three subgenomes. TaPHD genes were distributed in higher density on chromosomes 4 and 5. On the other hand, the TaC2H2 genes could only be localized on chromosomes 5B, 5D, 1, and 4 due to the low identification number, and the TaC3HC4 gene could not be identified on chromosome 4.

## 2.2. Multiple Sequence Alignment and Phylogenetic Analysis of TaZFPs

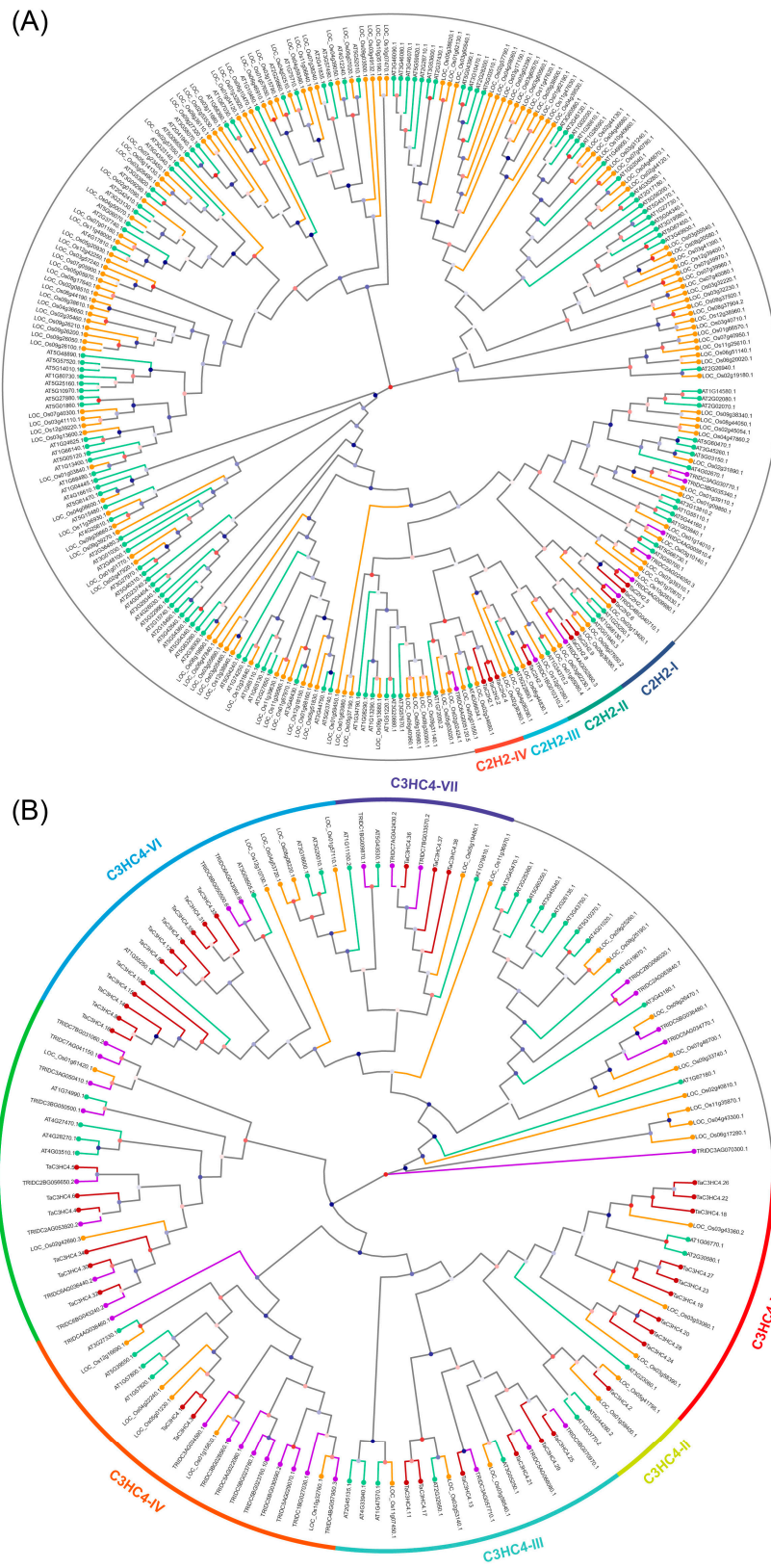
To explore the evolutionary relationships of the four TaZFP subfamilies, we performed multiple sequence alignment and phylogenetic analysis of all 269 TaZFP amino acid sequences with those from *A. thaliana*, *Triticum dicoccoides*, and *Oryza sativa*, respectively, using the subfamilies as a taxonomic basis. After that, several unrooted phylogenetic trees were constructed using Heuristic Neighbor-Joining (HNJ) and 1000 Shimodaira-Hasegawa (SH) tests, including four subfamily gene evolutionary trees from *T. aestivum*, *A. thaliana*, *T. dicoccoides*, and *O. sativa* (Figure 2). Moreover, an evolutionary tree of gene subfamilies was constructed using all TaZFPs. The specific genes and numbers are shown in Table S2. According to the tree's topology and the defined classification of the *A. thaliana* ZFP subfamilies, the phylogenetic trees of C2H2, C3HC4, CCCH, and PHD proteins from the four species were divided into several subgroups of 4, 7, 12, and 14, respectively. These results were similar to the findings of Sun et al. [26,27].

Among the identified phylogenetic subgroups, the PHD-IV subgroup contained the most significant number of TaPHD genes, accounting for 18.88% of the total number of TaPHD genes, followed by the CCCH-X subgroup containing 16 members, accounting for 20.25% of the total number of TaCCCH genes. In the C3HC4 gene phylogenetic tree, C3HC4-VI and C3HC4-I were the largest TaC3HC4 subgroups, accounting for 28.95% and 23.68%, respectively. The C2H2-III subgroup, with only one member, was the smallest taxon. In addition, there were inconsistent clusters of members of TaC2H2, TaC3HC4, and TaPHD with genes from *A. thaliana*, *T. dicoccoides*, and *O. sativa*, especially the TaC2H2 gene, that was absent in other subgroups, suggesting some changes in the C2H2 gene during the evolution of different species.



**Figure 1.** Syntenic relationships, chromosomal localization, and distribution of the *TaZFP* gene. (A) Red represents TaC2H2; purple represents TaC3HC4; green represents TaCCCH; orange represents TaPHD. The outer rectangles represent chromosomes and show roughly the physical location of the 269 *TaZFP* genes. The heat map of the middle rectangle indicates the gene density at the corresponding chromosome position; the grey lines in the inner background indicate col-linear blocks of *T. aestivum*; the other coloured lines indicate segmented repeat gene pairs. Tandem repeat gene pairs are located adjacent to each other and marked. (B) Distribution of the number of *TaZFP* genes on 21 chromosomes. Chromosomes from subgenomes A, B, and D are indicated in green, orange, and purple, respectively.





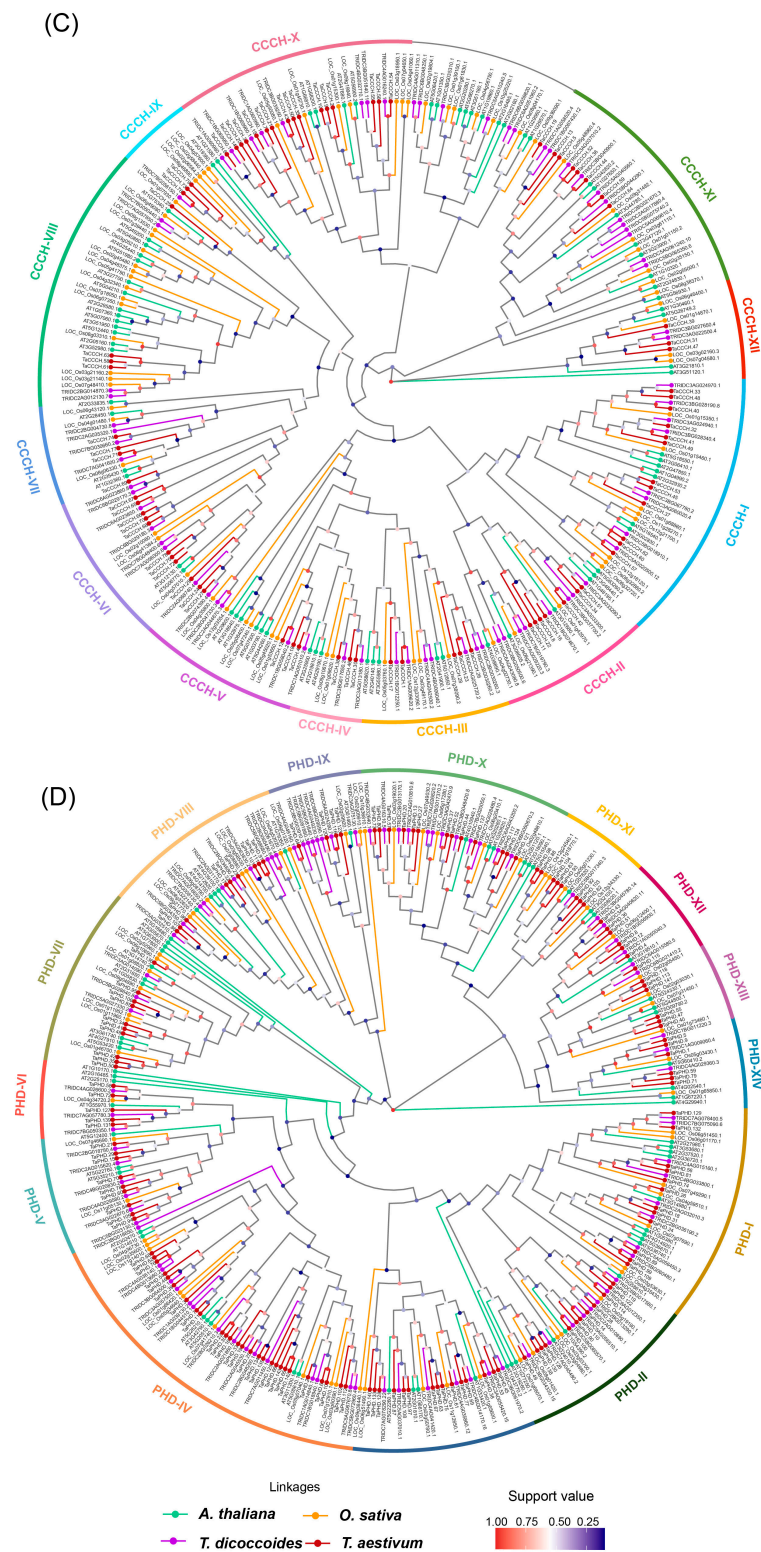


**Figure 2.** Phylogenetic trees of ZFP subfamily genes in *T. aestivum*, *T. dicoccoides*, *O. sativa*, and *A. thaliana*. (A) C2H2. (B) C3HC4. (C) CCCH. (D) PHD. Each identified subgroup is marked with Roman numerals near the branch. The different colours on the terminal branches represent ZFP genes from different species. The colours of nodes are a mapping of support values from 1000 SH tests.

### 2.3. Gene Duplication, Synteny, and Ka/Ks Analysis of TaZFPs

Synthetic analysis is routinely used to track the evolutionary relationships of plant gene family members. Synthetic analyses were performed within the *T. aestivum* genome using MCSanX and TBtools. Table S4 shows the syntenic relationships of homologous pairs in TaZFPs. The results indicated that 243 pairs (223 TaZFPs) out of 269 TaZFPs were caused by segmental duplication, and seven pairs (14 TaZFPs) were caused by tandem duplication events, which are highlighted on the chromosome of Figure 2. Furthermore, fragment replication played a dominant role in the evolution of TaZFPs. Most of the ZFP genes in other plants were also derived from segmental duplication, such as *Gossypium hirsutum* and *Phyllostachys edulis* [28,29]. As shown in Figure 2, paralogous chromosome groups 3 and 5 contain the largest number of segmentally duplicated gene pairs. The tandem duplicated gene pairs, which mainly originate from subgenomes A and D, have the highest frequency and coverage of 91.61% in the TaPHD.

To further explore the evolutionary origins of the ZFP subfamily members between *T. aestivum* and other closely related species, we constructed a synteny map with *T. dicoccoides*, *O. sativa*, and *A. thaliana* based on orthologous gene pairs, with identified numbers 531, 239, and 20, respectively (Figure 3 and Table S5). The number of TaZFPs identified as homologous after de-duplication was 239, 172, and 19, respectively. In the three subgenomes of *T. aestivum*, 251 segmental duplicated gene pairs were identified (71 between subgenomes A and B, 79 between subgenomes A and D, and 75 between subgenomes B and D). This number is smaller than the number of orthologous gene pairs between *T. aestivum* and the subgenomic donor (*T. dicoccoides*).

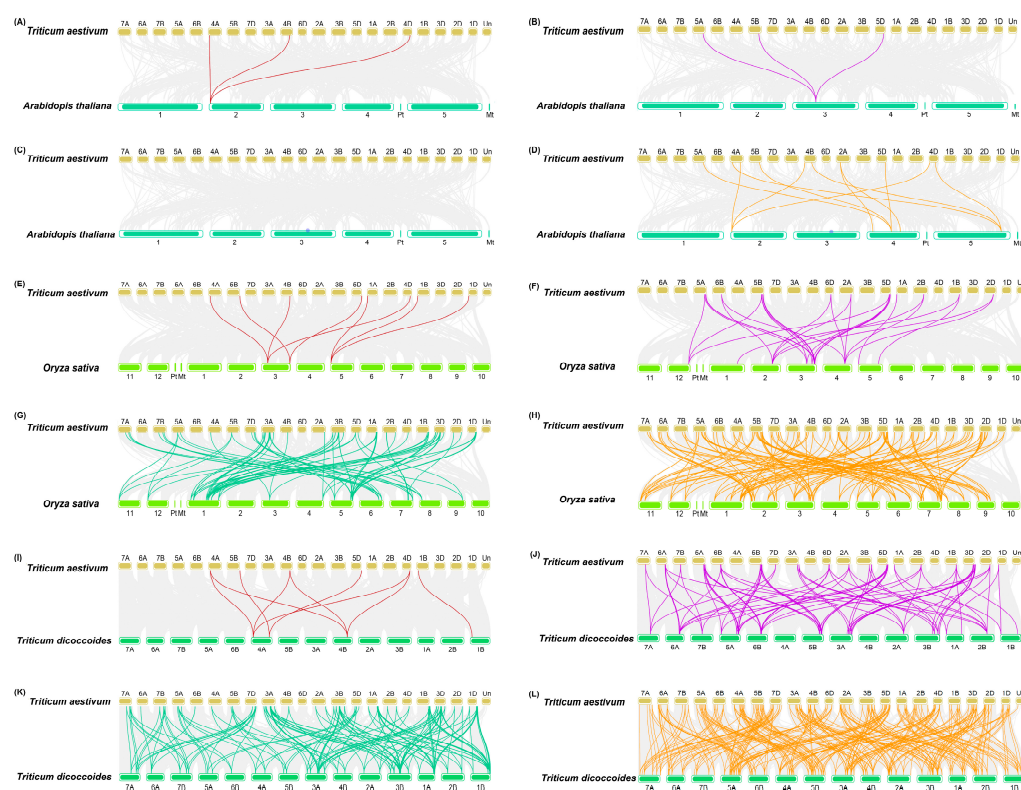


**Figure 3.** Genome-wide synteny relationship of TaZFPs orthologous with three representative plants' viz., (A–D) *A. thaliana*, (E–H) *O. Sativa*, and (I–L) *T. dicoccoides*. The grey line in the background indicates the syntenic region of *T. aestivum* and other plant genomes. The other coloured lines indicate different gene pairs, the red line indicates the co-linear TaC2H2 gene pair, the purple represents TaC3HC4, the green represents TaCCCH, and the orange represents TaPHD.



Since the ratio of  $K_a/K_s$  is a good indicator of the selection pressure occurring at the protein level, we evaluated the values of  $K_s$  (synonymous) and  $K_a$  (nonsynonymous) as well as the ratio of  $K_a/K_s$  (Table S4).  $K_a/K_s < 1$ ,  $K_a/K_s = 1$ , and  $K_a/K_s > 1$  generally indicate negative, neutral, and positive selection, respectively [30]. A total of 240 segmental duplicated gene pairs had  $K_a/K_s < 1$ , ranging from 0 to 0.94, with mean values of  $K_a$ ,  $K_s$ , and  $K_a/K_s$  of 0.06, 0.22, and 0.28, respectively. Among them, five tandem duplicated gene pairs had  $K_a/K_s < 1$ , ranging from 0.47 to 0.93, and the mean values of  $K_a$ ,  $K_s$ , and  $K_a/K_s$  were 0.1, 0.16, and 0.91, respectively. The time span of the replication-derived *TaZFPs* was 0 to 128.1Mya (millions of years ago), with 76.21% of the sequences having a duplication-derived time of less than 30 Mya. This is compatible with the temporal distribution at the subfamily level. Meanwhile, the remaining part of the sequence is mainly from TaPHD and TaCCCH.

#### 2.4. Gene Structure and Conserved Motifs of Four *TaZFP* Gene Subfamilies

We observed that intronless genes are most abundant in the TaCCCH, followed by the TaC2H2 and TaC3HC4. TaPHD.95 and TaPHD.106 contain 25 introns, the highest content among four *TaZFP* subfamilies. A small part of genes in the TaPHD have very large introns and very short exons, e.g., TaPHD.23 is 45,156 bp long, while the protein length is only 218 aa.

To reveal the structural variation of the *TaZFPs* in *T. aestivum*, the MEME program and SMART server were used to predict the conserved motifs present in *TaZFPs*, and a total of 12 motifs were identified (Figure S2). The results show that motif A contains Cys(2)His(2) (C2H2) residues, enabling it to form a short  $\beta$  hairpin and an  $\alpha$ -helix ( $\beta/\beta/\alpha$  structure) to bind to the DNA major groove and recognize the DNA sequence through the short  $\alpha$ -helix [31]. The motif D with 40 to 60 residues and a cysteine spacing of C-x(2)-C-x(9-39)-C-x(1-3)-H-x(2-3)-C-x(2)-C-x(4-48)-C-x(2)-C was identified as the ring-finger conserved domain of the C3HC4 protein. The motif G has the typical C-x8-C-x5-C-x3-H structure, which is thought to be a conserved structural domain of CCCH proteins, and motifs J and L are both typical motifs of PHD proteins. Motif K of 27 TaPHD proteins was identified as an Alfin domain that explicitly recognizes the trimethylated H3 tail on 'Lys-4' (H3K4me3), while other motifs were identified as conserved sequences [32]. In addition, the RRM structural domain of the bound RNA was identified in eight proteins (TaCCCH.63, TaCCCH.5, TaCCCH.58, TaCCCH.13, TaCCCH.61, TaCCCH.44, TaCCCH.25, TaCCCH.52). A large number of domains related to histone binding, DNA binding, and chromatin activity regulation were also identified in TaPHD, such as BAH, BRCT, ING, HOX, SET, SAP, etc. Notably, TaC2H2 and TaCCCH are commonly present with multiple characteristically conserved domains with a repeat count of 2-7 and a few TaPHDs (TaPHD.24, TaPHD.35, TaPHD.50, TaPHD.70, TaPHD.74, TaPHD.126, TaPHD.130, TaPHD.138, etc.) also have the phenomenon, where the number of repetitions is three. This duplication and extension of the finger-like structural domain contribute to DNA-zinc finger protein interactions [33,34]. Overall, the *TaZFPs* have high structural intron diversity, and the corresponding protein identifies the zinc finger motif.

#### 2.5. Stress-Related Cis-Acting Regulatory Elements (CAREs) of the *TaZFP* Gene Promoter

The 2kb upstream promoter region of four *TaZFPs* subfamilies members was extracted and analyzed using PlantCARE online software to investigate their evolutionary and functional differences. A total of 40 abiotic stress response-related Cis-acting regulatory elements (CAREs) were identified in the *TaZFPs* (Table S6), with TaC2H2, TaC3HC4, TaCCCH, and TaPHD predicting 26, 30, 35, and 37 motifs, respectively. CAREs involved in the light response are most abundant and prevalent in the *TaZFP* gene subfamily (Figure 2). These genes are upstream of multiple CAREs (e.g., G-box, P-box) that bind transcription factors (e.g., MRE) and phytohormones. This suggests that *TaZFPs* may be cross-regulated with other proteins and play a crucial role in light responses that are co-regulated by phytohormones and multiple transcription factors. In addition, many CAREs are involved in abiotic



stress or environmental stress response processes such as low temperature, hypoxia-specific induction, and anaerobic induction, such as ARE, DRE, GC-motif, and LTR [35–38]. The numbers of these are shown in Figure 4. These environmental stress-related CAREs were found in the promoter regions of the ZFP genes of the C2H2 type in *S. tuberosum*, the CCCH type in *Solanum lycopersicum*, the C3HC4, and the PHD type in *Capsicum annuum* [13,39–41]. The distribution of CAREs on genes is shown in Figure S3.

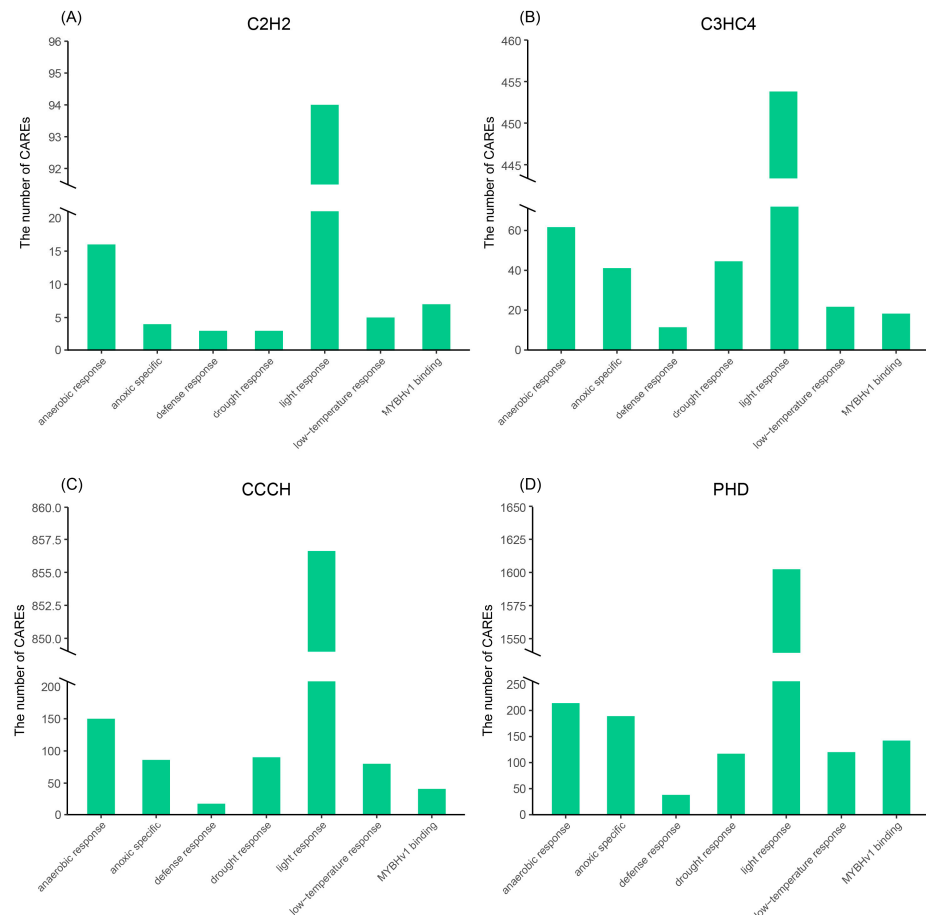


**Figure 4.** The most common *cis*-acting regulatory elements of the different *TaZFP* subfamilies. (A) TaC2H2 (B) TaC3H4 (C) TaCCCH (D) TaPHD.

## 2.6. Gene Ontology (GO) Enrichment and Protein-Protein Interaction Network of *TaZFPs*

All *TaZFPs* were successfully annotated and assigned GO terms (Table S7). The enrichment results of the agriGO database showed that the annotation of the biological process category was the central part. The GO terms in the biological process category relate to processes such as growth and development, stress response, and hormone regulation, including plant organ development (GO:0099402), regulation of development, heterochronic (GO:0040034), response to water deprivation (GO:0009414), regulation of response to water deprivation (GO:2000070), regulation to freezing (GO:0050826), and regulation of salicylic acid metabolic process (GO:0010337). In the molecular function category, the majority of the *TaZFP* subfamily was enriched in zinc ion binding (GO:0008270), followed by a majority enriched in nucleic acid binding (GO:0003676) (Figure 5). The cellular component category showed enrichment mainly in the intracellular membrane-bounded organelle (GO:0043231) and nucleus (GO:0005634). Similar GO annotation content was observed for the ZFP genes of *C. sativus*, *Brassica napus*, and *C. annuum* [22,41,42].

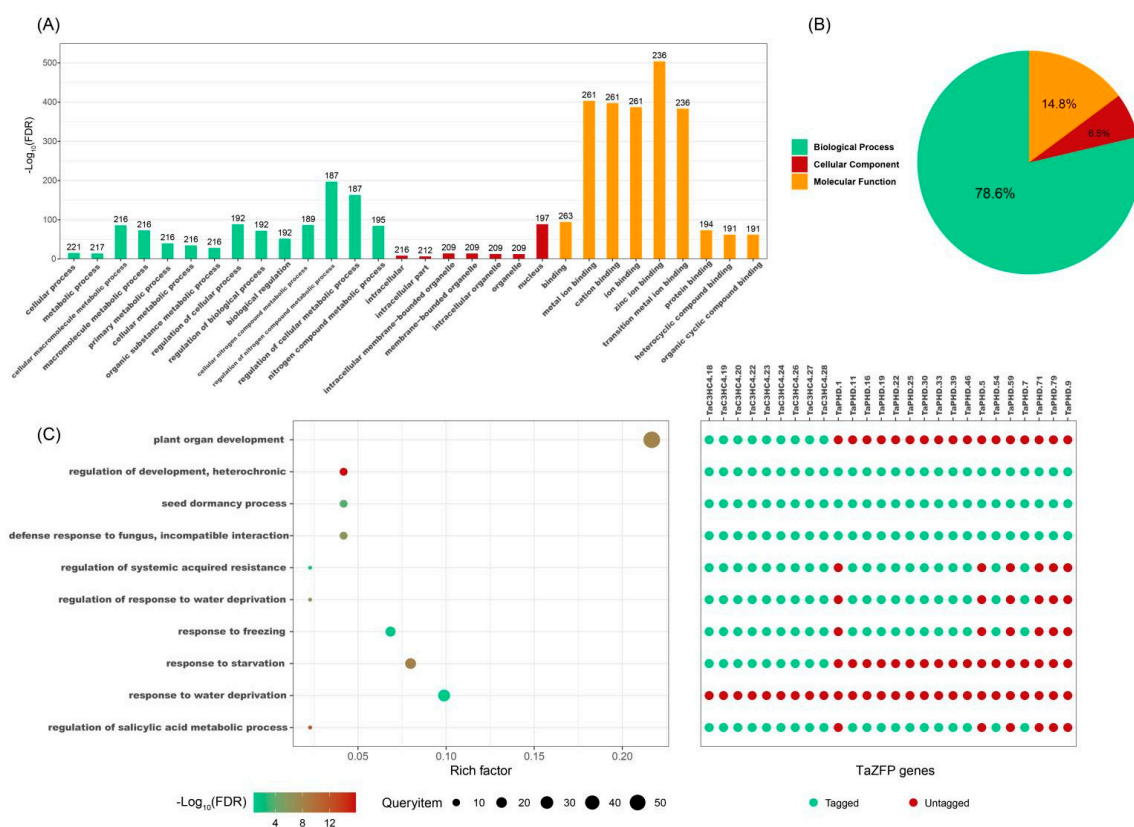


**Figure 5.** Gene ontology (GO) enrichment analysis of 269 *TaZFPs* under drought stress. (A) Top thirty most annotated GO items. (B) The proportion of different GO annotations. The cut-off value is  $FDR \leq 0.05$  for 501 GO entries. (C) Representative *TaZFPs* are assigned to categories related to development, stress, and hormone response and regulation. Green circles indicate that the gene does not belong to this category; red circles indicate that the gene belongs to the relevant category; the colour gradient indicates the size of the  $-\log_{10}(FDR)$  value; the size of the circle indicates the number of *TaZFPs*; the ‘Rich factor’ refers to the number of *TaZFPs* as a proportion of the total number of genes.

We selected 10 representative biological processes shown in Figure 5 below, including growth and development, stress response, and hormone regulation. The 26 proteins with response to water deprivation annotation were searched in the other nine biological processes to see whether they simultaneously functioned in more than one biological process. The results showed that 17 of the 26 proteins involved in response to water deprivation possessed both regulation of response to water deprivation, i.e., both response and positive regulation of response to water deprivation [43]. At the same time, these 17 proteins are also involved in plant organ development. In regulating systemic acquired resistance, regulation of water deprivation, response to freezing, and regulation of the salicylic acid metabolic process, there are six identical proteins, TaPHD.1, TaPHD.5, TaPHD.9, TaPHD.59, TaPHD.71, and TaPHD.79. It is tentatively assumed that these six proteins will likely play essential roles in growth and development, stress response, and hormone regulation. However, it should be noted that the 26 selected proteins were not associated with the regulation of development, heterochronic, and GO records.

Protein interaction analysis and hierarchical clustering results showed that eight *TaZFPs* interact in six classes and five relatively independent networks, with members of all four ZFP subfamilies involved (Figure 6). TaPHD members, which occupy the central part of the most complex network, still play an important role, with a total of 23 proteins covering four ZFP subfamilies interacting and acting on more than 10 objects. Among them, there are several proteins with identical targets, e.g., TaPHD.4, TaPHD.8, TaPHD.12,

TaPHD.36, TaPHD.43, TaPHD.51, and TaPHD.115 all interact with their nearby TaPHD.100, TaPHD.110, and TaPHD.140.

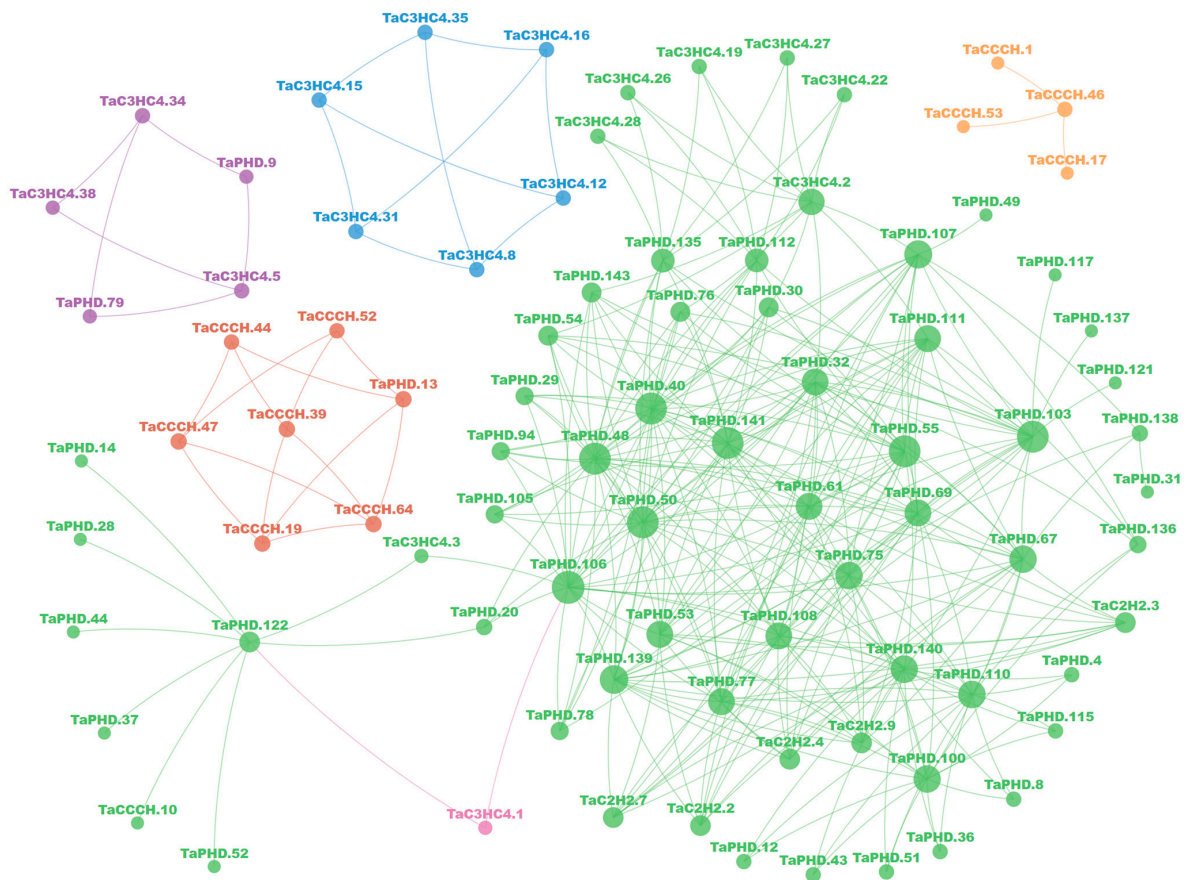


**Figure 6.** Putative interaction network of TaZFPs in *T. aestivum*. A total of 366 interactions are shown between 88 TaZFPs. The size of the circle is a mapping of the number of interacting objects. The colour of the circle represents the clustering category to which it belongs.

### 2.7. Expression Pattern Analysis of TaZFPs under Abiotic Stresses

To investigate the tissue-specific expression patterns and functions of TaZFPs in *T. aestivum* under abiotic stress, we performed expression profiling in different tissues under drought stress (DS) and heat stress (HS) treatments (Figure 7 and Table S8) [44]. The results showed that most TaZFPs were highly expressed in seedling leaves while exhibiting tissue-specific expression patterns that were detectable in leaves, roots, and grains, except for 17 genes that were not expressed within either data set. Genes with little or no expression were concentrated in the TaC2H2-I, TaCCCH-X, TaPHD-IV, and TaPHD-XI subgroups. Meanwhile, some members of TaC3HC4-V, TaCCCH-I, TaCCCH-III, TaCCCH-XI, and TaPHD-IV were consistently expressed at high levels in all three tissues. Among them, the TaPHD-IV subpopulation contained very low or no expression and higher expression levels of the members. In *T. aestivum* seedling leaves, the expression of 149 genes increased after DS-1h, and 53 of them (e.g., eight genes from TaCCCH-I, six from TaCCCH-VI, six from TaCCCH-X, etc.) continued to increase at DS-6h. Whereas 52 genes were up-regulated under both HS-1h (eight PHD-III, seven CCCH-X, etc.) and DS and HS-1h (eight PHD-III, six CCCH-X, etc.), and there was an overlap of 41 genes (six PHD-III, six CCCH-VI, six CCCH-X and all five members from CCCH-III, etc.). After 6 h, the number of genes up-regulated under HS and DS, and HS treatment increased, and all 139 were up-regulated (all 13 members from PHD-X, 11 PHD-III, 10 PHD-VI, etc.). Meanwhile, a significant amount of ZFP genes were down-regulated under DS treatment relative to the susceptible variety Atay85. Only 27 of these genes were up-regulated in expression, mainly involving PHD and



CCCH genes, and did not contain members of the C2H2 subfamily. The resistant variety Zubkov had 191 genes with up-regulated expression under the leaves (e.g., TaCCCH-I, TaPHD-IV, TaC3HC4-I, TaC3HC4-VI, and most subgroup members). This marked difference in expression was also present in root tissue. Varietal expression pattern differences in the grain remained. In contrast, the number of genes up-regulated in response to expression was much higher in the grain of Atay85 than in that of Zubkov. The differential expression patterns of *TaZFPs* under HS and DS, and HS treatments were also similar in root and grain tissues of both species. However, most genes were up-regulated in leaf tissues under DS and HS treatment, and the level and number of genes up-regulated were greater in Atay85 than in Zubkov.

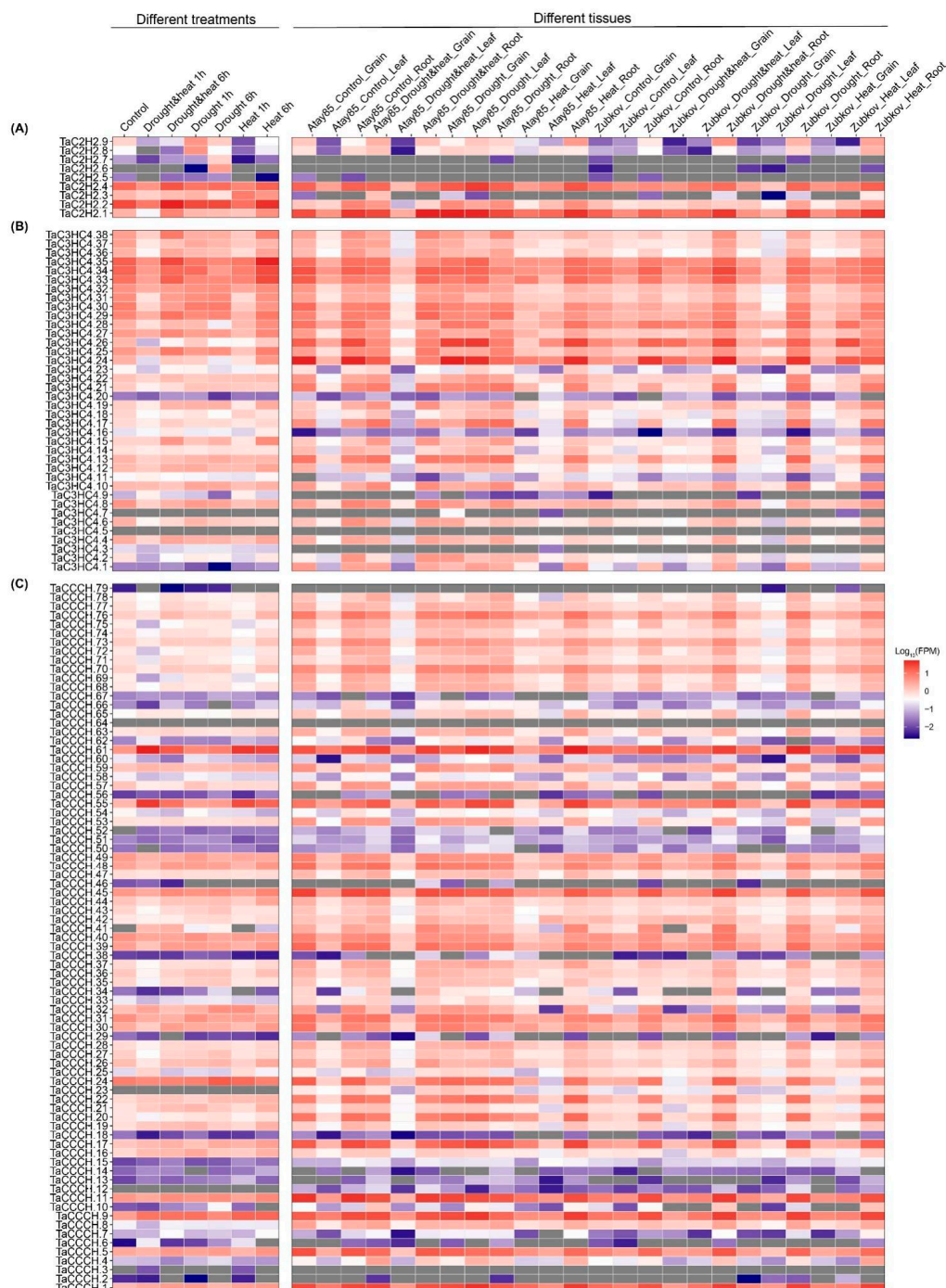
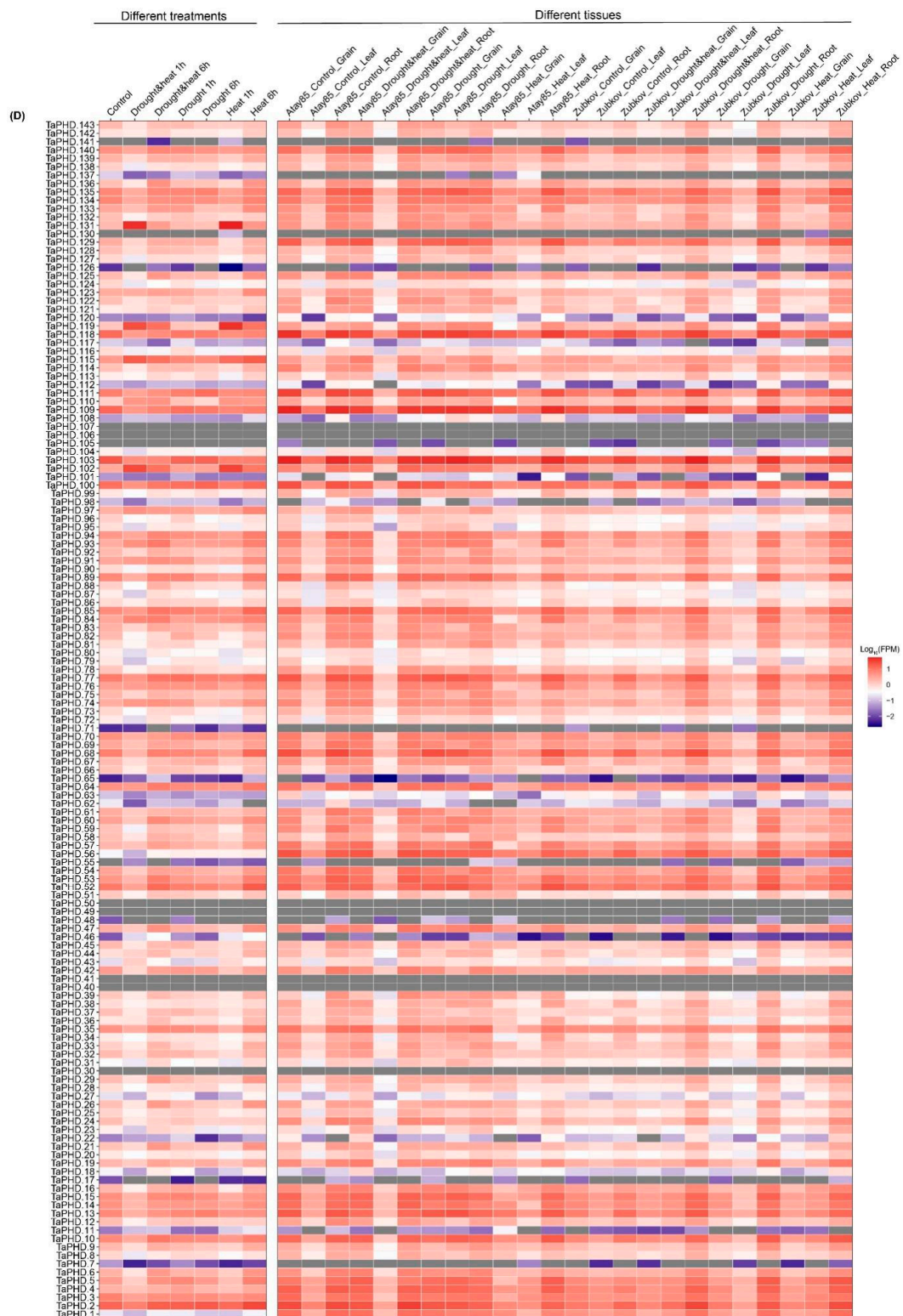


Figure 7. Cont.





**Figure 7.** TaZFP gene expression levels heatmap at different treatment times and tissues under drought stress. TPM values were scaled by the logarithm of the base 10 to form the heatmap. (A)TaC2H2 (B) TaC3HC4 (C) TaCCCH (D) TaPHD.

To confirm expression patterns of *TaZFPs* from transcriptome data, 10 *TaZFPs* were selected based on GO enrichment and expression profiling results. Their expression levels in seedling leaves under drought treatment were analyzed using qRT-PCR experiments

(Figure 8). Except for *TaC3HC4.20*, the relative expression levels of nine genes were increased in DS-3d and DS-6d treatment. Among them, six genes from the PHD-VI subgroup (Figure 8D–G,I) showed similar differential expression patterns. Their relative expression levels increased by at least 10 times under DS-3d treatment and about 5 times after DS-6d treatment. The expression levels of *TaCCCH.1* and *TaPHD.62* were the same as those of reference genes under DS-3 d but increased at DS-6 d. Based on the results of qRT-PCR, the expression profiles of the 10 *TaZFP*s were generally consistent with previously published data.

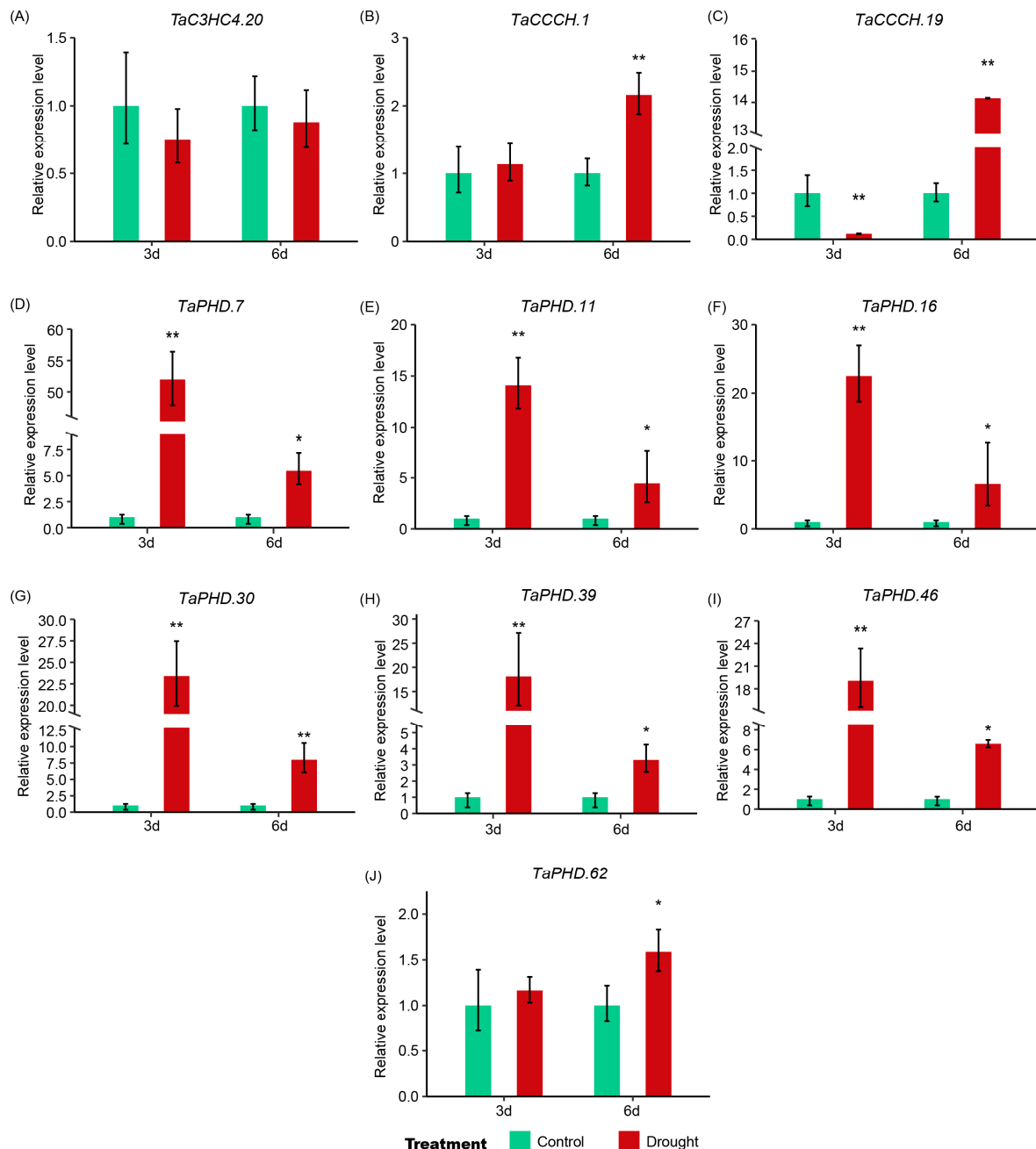


**Figure 8.** The relative expression levels of *TaZFP* genes after 3-day (3d) and 6-day (6d) drought treatments were examined by qRT-PCR. The *T. aestivum* actin gene was used as an internal reference control. Relative expression levels are the mean  $\pm$  SE of the three samples, with significant differences marked as (\*)  $p < 0.05$  and (\*\*)  $p < 0.01$  under the *t*-test. (A) *TaC3HC4* (B) *TaCCCH.1* (C) *TaCCCH.19* (D) *TaPHD.7* (E) *TaPHD.11* (F) *TaPHD.16* (G) *TaPHD.30* (H) *TaPHD.39* (I) *TaPHD.46* (J) *TaPHD.62*.

### 3. Discussion

ZFP transcription factors are widespread in the plant kingdom and play an instrumental role in plant growth, development, and response to environmental stress. ZFPs have been identified in many plant species [5,45,46]. However, no systematic studies have been reported on the four TaZFP subfamilies of *T. aestivum*. As a widely grown cereal crop, *T. aestivum* has significant economic and agricultural values. Uncovering the characterization of the TaZFP gene family under abiotic stress is essential for further understanding and improving the resistance of *T. aestivum*. In this study, 9 TaC2H2, 38 TaC3HC4, 79 TaCCCH, and 143 TaPHD were identified. Subsequently, their physicochemical properties, phylogenetic relationships, gene duplications, gene structure, conserved structural domains of peptide sequences, stress-related CAREs, GO annotation, protein-protein interactions, and expression profiles under DS and HS were analyzed.

Physicochemical properties are these functional proteins' most fundamental and crucial characteristics [26]. We have analyzed the physicochemical properties of TaZFPs and predicted the protein sequence's length, molecular size, and isoelectric point. The projections are consistent with the results for *S. lycopersicum* and *P. edulis* [39,47]. The higher hydrophilicity may be related to these proteins' high number of repeats and the need for a finger-like structural domain for binding to nucleic acids. Four subfamilies have high diversity in length, isoelectric point, and instability, suggesting they may have a diverse functional subgroup classification. These polymorphisms within four gene subfamilies may be a prerequisite for the diversity of physiological functions in which TaZFPs are involved, i.e., the existence of differential responsive regulation by different members of the same subfamily [11,12].

The chromosomal localization results showed that TaZFPs were evenly distributed across the three subgenomes of *T. aestivum* but at varying densities on the chromosomes. On the subgenomic levels, this may lead to genes with redundant functions, suggesting that some TaZFPs may have undergone gene loss events during evolution, subjecting to low purifying selection. Meanwhile, this uneven distribution of ZFP is also typical in other plants such as maize and *S. lycopersicum* [39,48]. Some studies attribute this differential localization to gene duplication patterns. As a result, genes from the same family are distributed in different chromosomes to achieve full function [49].

Based on phylogenetic analysis, TaC2H2, TaC3HC4, TaCCCH, and TaPHD proteins were classified into 4, 7, 12, and 14 subgroups, respectively. The distribution of motifs of members of the same subfamily tends to be more highly conserved. The differential grouping of motif composition combined with the results of phylogenetic analysis supports the reliability of group classification and suggests that TaZFPs in different groups may be functionally divergent. The results of the TaZFP evolutionary branching of TaZFP are consistent with four TaZFP subfamilies' phylogenetic clustering, further supporting the evolutionary relationship between each TaZFP member. It has been reported that the functions of homologous genes can be inferred from the phenotypes of highly homologous genes from *A. thaliana* [50,51]. The 31 groups in our study (37 groups in total) are supported by previous high introductory studies (Table S3). For example, DRIP1 and DRIP2, which are homologous to nine members of the C3HC4-I subgroup, are involved in regulating stress-related transcriptional changes and drought resistance. In *A. thaliana*, atU2AF35b and atU2AF35b, which are orthologous to the CCCH-XI subgroup, are important splicing factors localized in the nucleus and cytoplasm as U2 auxiliary factor small subunits and have a vital role in recognition of the 3'-splice site [52]. Altered expression levels can lead to pleiotropic traits such as late flowering, abnormal leaf morphology, and flower and angular fruit shape [53]. On the other hand, whether C3HC4-I and CCCH-XI subgroups are drought-resistant needs to be further verified.

It is worth mentioning that all TaC2H2s are located in the same large branch in the C2H2 protein evolutionary tree and are missing in other branches (Figure 2). Genes clustered in branches of the phylogenetic tree are generally considered to be conserved in their evolutionary status [26]. Considering that this conserved feature is also found in plants

such as *Camellia sinensis*, *O. sativa*, etc., it can be assumed that TaC2H2 has evolutionary conservatism [54,55]. Furthermore, consistent with the evolutionary closeness of the four species, ZFP genes from *T. dicoccoides* were the most clustered with TaZFPs, followed by *O. sativa*. Regarding the number of ZFPs, it was found that the number of genes in *A. thaliana* and *O. sativa* was 26 and 35, respectively, more than that in *T. aestivum*, while the number of genes in *T. dicoccoides* was 64. Among them, the difference in the number of C3HC4 and CCCH genes between species was slight, while the number of C2H2 genes in the other three species was much more than that of *T. aestivum*, and the number of PHD genes was significantly less than that of *T. aestivum*. Despite the considerable variation in genome size and the number of genes encoded between the four species, the number of gene subfamilies encoding CCCH is similar. This may be because some of the CCCH genes became highly functionally differentiated during expansion and evolution earlier than the differentiation time in monocots and dicots [56]. In comparison, PHD members showed substantial expansion and functional divergence relatively late in most subgroups. The four TaZFP gene subfamilies in *T. aestivum* have been subjected to differential selection for intensity during evolution, and further gene duplication analysis is required.

Gene duplication events are an important source of gene novelty and a significant influence on the expansion of gene families that aggregate into gene families that facilitate the adaptation of plants to a wide range of current environmental challenges. There are four types of duplication: segmental duplication, tandem duplication, whole genome duplication, and trans-poson-induced duplication [57,58]. Gene duplication analysis showed that the fragment repeats that had dominated the evolution of the four TaZFP subfamilies, in particular, have contributed significantly to the massive expansion of the TaPHD family in *T. aestivum*.

Moreover, the syntenic analysis revealed that *T. aestivum* has varying degrees of orthologous relationships with members of the ZFP subfamily of three other closely related species. Among them, the number of orthologous gene pairs between *T. aestivum* and *T. dicoccoides* even exceeded the number of paralogous gene pairs between subgenomes of *T. aestivum*. Given the high degree of evolutionary homology between the two species and the greater number of duplicated genes compared to those within the subgenome, it can be inferred that this phenomenon is associated with polyploidy and gene loss, or chromosomal recombination, during evolution [59,60]. In addition, the orthologous genes of 14 TaZFPs in *T. aestivum* were observed in the other three species, indicating that these genes are relatively conserved during evolution. Nevertheless, in addition to 14 evolutionarily highly conserved orthologous genes identified in all four species, some of the identified TaZFPs are only synthetically related to genes in one species. For example, 24 TaZFPs were covalently related to *T. dicoccoides* (C2H2:1, C3HC4:3, CCCH:9, PHD:11). This implies that TaZFPs, especially PHD and CCCH, may have been lost and retained in the remaining two plants in *T. aestivum* and *T. dicoccoides*. Furthermore, this phenomenon could further explain the high homology of ZFP genes between them. Additionally, the number of paralogous gene pairs corresponding to the same gene between genomes in *T. aestivum* was generally 1–2 times. In comparison, it was maintained mainly above 3 times in the other three species, suggesting that four TaZFP subfamilies may have undergone a stronger selection pressure during its evolution in *T. aestivum* [45].

Paralogous and orthologous synthesis analyses suggest that the evolution of TaZFPs is dominated by segmental duplication events and may be subject to strong selection. Segmental duplex gene pairs account for a significant proportion of the evolution of the four TaZFP gene subfamilies. The results for Ka/Ks further validate that most duplicated genes, especially segmentally duplicated gene pairs, underwent strong purifying selection to reduce deleterious mutations, thus maintaining this gene subfamily's size and possible expression. This is consistent with the results of other plants, such as *Brassica rapa* and *Panax ginseng* [33,61].

The structure of a gene determines its coding potential and can also suggest the ancestry of the gene. This is because structurally similar genes may have evolved from a



common ancestor [62,63]. Introns are essential components of genes and play an important role in gene expression regulation and stabilization through intron-mediated enhancers, selective splicing, and increased efficiency of natural selection [64]. What can be found is that most *TaZFPs* have introns and a high diversity of features, such as the number, length, and distribution of introns (Figure S1), which may be caused by intron deletion and insertion events. Deshmukh et al. showed in rice that the mRNA produced by transcription of intron-rich genes might have higher stability [65]. The expression levels of these genes with long introns may be positively affected.

*Cis*-acting regulatory elements (CAREs) are short DNA sequences found on promoters. They regulate gene expression and are essential to the gene regulatory network. On the other hand, these non-coding DNA fragments also provide an idea about physiological processes, suggesting specific genes that may be involved [66,67]. For instance, PbrMYB21 can interact with the MYB-recognizing *cis*-element in the promoter region of PbrADC to regulate polyamine synthesis by modulating ADC expression levels, thereby altering the drought tolerance of *Pyrus betulaefolia* [68]. The observation of these CAREs by four *TaZFP* gene subfamilies suggests that *TaZFP* plays a vital role, mainly in light and abiotic stress responses. The importance of light in plant growth and development has been demonstrated. It is proposed to influence light-regulated trans-acting factors through the transduction of light signals and its binding to *cis*-acting elements in gene promoters to facilitate transcription in response to light. Directly or indirectly, this abiotic factor regulates the development and differentiation of plant cells [69,70]. In this study, a total of 32 species of 2927 light response-related CAREs identified from the upstream 2 kb fragment of the *TaZFP* gene indicate the critical involvement of *TaZFPs* in plant growth and development. Meanwhile, a total of 249 MBS were identified for 143 *TaZFPs*, revealing that the transcription factor MYB is also involved in regulating drought inducibility [71]. Overall, many *cis*-acting elements associated with environmental stress and plant hormone responses were identified, suggesting that the four *TaZFP* gene subfamilies may be involved in multiple signalling pathways [72,73].

GO analysis provides the possible basic functions of genes in cells, i.e., biological processes, molecular functions, and cellular components. It has been widely used to determine the various functions of plant and animal genes [74]. Overall, these GO terms highlight four subfamilies of *TaZFPs* that function primarily in the nucleus and organelles within the cell membrane. They bind to nucleic acids through finger-like structures formed by chelation with  $Zn^{2+}$  and are involved in regulating several processes such as growth and development, abiotic stress responses, and hormonal regulation.

Protein-protein interaction prediction can reveal putative relationships among proteins. Interacting proteins may play important roles in plant growth, development, and response to various stresses through integrative regulation [75,76]. The interaction network shows several proteins with a high number of interactions. Among them, the Inhibitor of Growth (ING) transcription factors (TaPHD.100 and TaPHD.110) can bind unmodified to the lysine 4-trimethylated histone H3 (H3K4me3) [77]. Furthermore, TaPHD.140 with the PHD, JmjC, and PLU-1 structural domains may play a role in the histone demethylation machinery. They are hypothesized to play a key role in regulating functionally diverse protein networks [78].

Tissue-specific expression differences are one of the most critical indicators of functional differentiation among genes and facilitate the regulation of various physiological processes by eliminating their redundancy [79]. The expression profiles suggest that most *TaZFPs* are involved in multiple plant growth and development processes and have tissue-specific or preferential expression patterns. In particular, members from the TaC3HC4-V, TaC3HC4-VI, TaCCCH-I, TaCCCH-III, TaCCCH-VI, TaCCCH-X, TaCCCH-XI, TaPHD-III, TaPHD-IV, TaPHD-X, and TaPHD-VI subgroups. The level of *TaZFPs* expression was more positively regulated in leaf and root tissues under both abiotic stresses, DS and HS, than in grain tissues.

Drought is one of the important environmental stressors affecting *T. aestivum* growth and development, often leading to reduced *T. aestivum* yield [80]. Previous studies have shown that the ZFPs respond to various abiotic stresses. For example, double mutants of AT1G06770.1 (DRIP1) and AT2G30580.1 (DRIP2) are more tolerant to drought stress compared to wild-type *A. thaliana* [81]. *TaC3HC4.20* is orthologous to *Arabidopsis* DRIP1 and DRIP2 and is down-regulated under drought-6d treatment, suggesting that they may have similar functions under drought stress. They are capable of mediating DREB2A ubiquitination and targeting 26S proteasomal protein hydrolysis. Under dehydration treatment, they act as E3 ubiquitin ligases with reduced expression levels, delaying DREB2A-regulated drought-responsive gene expression and negatively regulating drought-responsive gene expression for seed germination and seedling growth while improving drought tolerance in transgenic *A. thaliana*. Moreover, *TaC3HC4.20* was found to have a *cis*-element MBS for drought-induced stress response, which supports our hypothesis [82]. Notably, The expression level of *TaCCCH.1* showed a 14-fold increase under 6-day drought treatment. *TaCCCH.1* is a member of the CCCH-XI subgroup and is homologous to atU2AF35b and atU2AF35b, which are key factors in recognizing the 3' shear site of the mRNA precursor [53]. Therefore, this phenomenon suggests that it plays an important role in maintaining physiological processes such as plant growth and development under drought stress. Overall, these results validate the involvement of TaZFPs in plant responses to drought stress.

#### 4. Materials and Methods

##### 4.1. Identification of TaTFPs in *Triticum aestivum*

The structural domain and sequence identification were used to identify the TaZFP gene subfamilies in *Triticum aestivum*. First, the protein family ID (C2H2: PF00096, C3HC4: PF00097, CCCH: PF00642, PHD: PF00628) corresponding to the structural domains of each of the four ZFP gene subfamilies was retrieved from Pfam (<http://pfam.xfam.org/>, accessed on 3 May 2022), and the Hidden Markov Model (HMM) files for all protein subfamilies were downloaded. All protein sequences of *T. aestivum* were obtained from the EnsemblPlants database (<https://plants.ensembl.org/index.html>, accessed on 5 May 2022) and used to perform HMM searches (E-value < 0.01) on the software TBtools against the local protein database [26,83]. The search results were initially screened by taking the same part of the sequence score and the domain score. For determination, sequences of the four AtZFP gene subfamilies of *A. thaliana* were obtained directly from the Phytozome database (<https://phytozome-next.jgi.doe.gov/>, accessed on 6 May 2022) [84]. The sequences were used as reference sequences for Blastp (E-value <  $10^{-10}$ ) to confirm the homologous sequence in *T. aestivum*, which are potential TaZFP gene subfamily candidates.

In summary, based on the results of the above two approaches, the NCBI CDD (<https://www.ncbi.nlm.nih.gov/Structure/cdd/wrpsb.cgi>, accessed on 8 May 2022) and the HMMscan (<https://www.ebi.ac.uk/Tools/hmmer/search/hmmscan>, accessed on 8 May 2022) were used to confirm the presence of the core domain of TaZFPs. Finally, the protein sequences were examined by manual screening, mainly by running Blastp on NCBI (<https://www.ncbi.nlm.nih.gov>, accessed on 13 May 2022) and Uniport (<https://www.uniprot.org/>, accessed on 13 May 2022). The above processes were performed with redundancy removal operations. The gene subfamily localization of TaZFP on chromosomes was obtained from the EnsemblPlants database. The names of Ta and corresponding ZFP gene subfamilies were used as naming prefixes. Then, the numbering was added in order of the position of the gene subfamilies on the chromosomes from the long arm to the short arm, respectively. The ExPASy-ProParam online tool (<https://web.expasy.org/protparam/>, accessed on 28 June 2022) is used to predict the physicochemical properties of TaZFPs.

##### 4.2. Multiple Sequence Alignment and Phylogenetic Analysis

Multiple sequence alignment of genes from four species, *T. aestivum*, *A. thaliana*, *O. sativa*, and *T. dicoccoides*, was performed separately according to the four ZFP subfamily

categories using ClustalW on Mega-X software. All analyses use the software's default parameters. Then, sequence alignment was trimmed by TBtools v1.098 (Chen, C.C., South China Agricultural University (SCAU), Guangdong, China) as input files for the FastTree program v2.1.11 to construct Heuristic Neighbor-Joining trees. After that, the Jones-Taylor-Thorton (JTT) model of amino acid evolution and 1000 times SH tests were performed in the process [85,86].

#### 4.3. Determination of Chromosome Distribution, Synteny, and Ka/Ks of 4 TaZFP Gene Subfamilies

Chromosomal location information and the tandem and segmental duplication of the *TaZFPs* were analyzed using TBtools, the multicollinearity scanning tool MCScanX and BLASTP [87]. Data were obtained from the genome of *T. aestivum* in EnsemblPlants and gff3 annotation files. Afterward, the chromosomal distribution, intra-, and inter-specific (with other 3 species) gene synteny of *TaZFPs* were visualized. Duplicate events with  $\geq 80\%$  sequence similarity were identified by the bidirectional blast. Tandem and segmented duplication events were distinguished based on distance and chromosome distribution [88].

To estimate the duplication events of *TaZFPs*, we calculated Ka and Ks values of *TaZFP* duplicated gene pairs using the TBtools. Subsequently, the Ks values were used to approximate the duplication events according to  $T = Ks/2\lambda \times 10^{-6}$  Mya, assuming a clock rate ( $\lambda$ ) of  $6.5 \times 10^{-9}$  for synonymous substitutions [89].

#### 4.4. Identification of Gene Structure, Conserved Motifs, and Cis-Acting Regulatory Elements

Intron and exon start and stop site information was obtained from the GFF3 annotation file of *T. aestivum*. The conserved motifs of the four *TaZFP* subfamilies were predicted using the Multiple Em for Motif Elucidation (MEME) website server (<http://meme-suite.org/index.html>, accessed on 17 May 2022), and the subfamily recognition motifs were retained. The specific parameters were set as follows: the number of sequence occurrences was any number of repetitions (anr), the motif width was 6-200 amino acids, and other default settings were maintained. Motifs prediction results confirm the type of conserved structural domains via the SMART server (<https://smart.embl.de/>, accessed on 21 May 2022) [90]. To obtain the CAREs of *TaZFPs*, a 2-kb segment upstream of each gene's transcription start site (TSS) was taken and used for prediction analysis using the PlantCARE database (<http://bioinformatics.psb.ugent.be/webtools/plantcare/html/>, accessed on 23 May 2022). Identified cis-acting elements are classified according to their function. Gene structure, conserved motifs, and cis-acting regulatory elements are analyzed and visualized by the tidyverse, ggplot2, and ggenes R packages.

#### 4.5. GO Enrichment and Protein Interaction Network Establishment

GO annotations of *TaZFPs* were analyzed on agriGO (<http://systemsbiology.cau.edu.cn/agriGOv2/index.php>, accessed on 27 May 2022), and enrichment results were visualized using R (3.9.0). Protein-protein interactions (PPIs) were predicted using STRING database 11.5 (<https://string-db.org/>, accessed on 29 May 2022) and displayed on SCImago Graphica Beta 1.0.18, where interaction networks were screened with the criterion of combined scores  $> 0.7$  [91]. The protein-protein interaction network of *TaZFP* was predicted with high confidence (0.700) and visualized using Cytoscape.

#### 4.6. Gene Expression Analysis

To analyze the expression pattern of the *TaZFPs* under different treatments and different tissues, processed expression data were obtained from *T. aestivum* Omics 1.0 (<http://wheatomics.sdau.edu.cn/>, accessed on 10 July 2022) [92]. Specifically, for the expression profiles at different treatment times, two biological replicates were obtained for leaf tissue of *T. aestivum* seedlings after 1 h and 6 h of DS and HS treatments using transcriptomic data reported by Liu et al. [44]. For the expression profiles at the tissue level under DS and HS treatments, high-throughput RNA seq data (accession number:

PRJNA358808) were used to analyze the differential expression patterns of leaf, root, and grain tissues of two cultivars (resistant and susceptible) under stress treatments (DS, HS, and DS+HS). The differential expression patterns of DS, HS, and DS+HSTPM (transcripts per million) values of the TaZFPs are shown in Table S8. Heatmaps were plotted by the R (3.9.0).

#### 4.7. Plants Material and Culture

Based on GO analysis and abiotic stress expression heatmap results, drought-treated *T. aestivum* leaves were selected as the primary abiotic stress study. The bread *T. aestivum* cultivar Jimai 22 was used throughout the study. The seeds were placed in 10 cm × 10 cm perforated pots and incubated in an incubator (22 °C, 60% RH, 400 PPM CO<sub>2</sub>, 8 h dark, 16 h light) until the *T. aestivum* grew to the three-leaf stage. The cut-off water treatment was used as drought stress, and seedlings under normal growth conditions (22 °C, watered) were used as control. Leaves from the 3-day and 6-day drought treatments were collected, frozen immediately in liquid nitrogen, and stored at −80 °C for further studies [26,93]. All experiments were performed in parallel with three biological replicates at each specific time point.

#### 4.8. RNA Extraction and qRT-PCR Analysis

Total RNA was extracted from each frozen sample using TRNzol Universal Reagent (Tiangen Biotech Co., Ltd., Beijing, China). cDNA synthesis was performed in one step according to the instructions of the TRUEScript 1st Strand cDNA Synthesis Kit (Aidlab Biotechnologies Co., Ltd., Beijing, China). Quantitative analysis was performed on a QuantStudio™ 1 Real-Time PCR Instrument (Applied Biosystems, Foster City, CA, United States) using TaKaRa TB Green™ Premix Ex Taq™ II (Takara Biotechnology Co., Ltd., Beijing, China) with a reference fluorescence of SYBR. According to a previous study, the actin gene was used as an internal control. Each reaction system was carried out in 25 µL of the mixture. The reaction mixture contained the following reagents: 1.0 µL cDNA, 2 µL of each primer pair, 12.5 µL SYBR, and 9.5 µL ddH<sub>2</sub>O. Gene-specific primers are shown in Table S9. qRT-PCR cycling parameters were 40 cycles at 95 °C for 15 s and 60 °C for 1 min, with a ramp-up and ramp-down rate of 1.6 °C/s. At the end of the reaction, samples were slowly heated from 60 °C to 95 °C at 0.15 °C/s, and melting curves were generated by continuous fluorescence monitoring. All reactions were repeated three times to ensure reproducible results. The qRT-PCR results were analyzed using the 2<sup>−ΔΔCT</sup> method to estimate ploidy changes in the expression levels of the genes of interest using 3-day and 6-day control treatments [94].

## 5. Conclusions

ZFPs, as one of the critical transcription factors, are involved in various physiological processes, such as seed development, plant growth, and biotic and abiotic stress responses. In this study, we investigated the physicochemical properties, phylogeny, chromosome distribution, gene duplication, covariance, gene structure, conserved motif, stress-related CAREs, GO enrichment, protein-protein interactions, expression patterns of 269 TaZFPs (9 TaC2H2, 38 TaC3HC4, 79 TaCCCH, and 143 TaPHD) in *T. aestivum*. TaC2H2, TaC3HC4, TaCCCH, and TaPHD genes were classified into 4, 7, 12, and 14 classes based on the phylogenetic tree constructed from ZFP genes of *T. aestivum*, *A. thaliana*, *T. dicoccoides*, and *O. sativa*, respectively, according to the ZFP subfamily classification. Meanwhile, we analyzed the number distribution and density heterogeneity of the four TaZFP subfamilies at subgenomic and chromosome levels. We identified 143 fragment duplication events and 7 tandem duplication events in TaZFPs, indicating that fragment duplication played a dominant role in the evolution of TaZFPs. Furthermore, the synteny analysis and Ka/Ks results between *T. aestivum* and the other three representative plants further indicated that four TaZFP gene subfamilies experienced strong purifying selection. Subsequently, four gene subfamilies were identified with specific motifs and diverse gene structures. Many



abiotic stress-related CAREs were identified in the promoters of *TaZFPs*. GO enrichment results showed that all *TaZFPs* were annotated under the nucleic acid binding and metal ion binding. The expression patterns indicated that some *TaZFPs* were involved in response to DS and HS. Overall, this study provides comprehensive information on the sizeable *TaZFP* gene subfamilies, rarely studied on a subfamily scale, and will help identify particular *TaZFP* gene functions in further studies. Further, the characterization of this *T. aestivum* gene family, which is highly responsive to drought and heat, will undoubtedly provide new theoretical support and inspiration at the molecular level for use in agriculture, ecosystem studies, modelling, and other fields.

**Supplementary Materials:** The following supporting information can be downloaded at: <https://www.mdpi.com/article/10.3390/plants11192511/s1>, Figure S1: Phylogenetic tree, gene structure, and conserved motifs of *TaZFPs*. Figure S2: Conserved motifs of *TaZFPs*. Figure S3: *Cis*-acting regulatory elements of *TaZFPs*. Table S1: Details of the identified *TaZFP* genes. Table S2: Members of four *TaZFP* subfamilies phylogenetic tree. Table S3: Putative functions of the *TaZFP* in *T. aestivum*. Table S4: *Ka/Ks* ratios and divergence times of gene pairs in *T. aestivum*. Table S5: Orthologous pairs between *T. aestivum* and other plants. Table S6: *Cis*-acting regulatory elements (CAREs) in the promoter of *TaZFP* genes. Table S7: Gene ontology of the *TaZFP* genes in *T. aestivum*. Table S8: The expression levels of *TaZFP* genes of *T. aestivum* under drought stress. Table S9: Primer sequences for qRT-PCR.

**Author Contributions:** Conceptualization, Z.W., S.S., Y.W. and P.Y.; Data curation, Z.W., S.S., Z.Z., X.H. and P.Y.; Formal analysis, Z.W. and S.S.; Funding acquisition, P.Y.; Investigation, Z.W., S.S., Y.W., W.T., Z.Z., X.H. and P.Y.; Methodology, Z.W., S.S. and P.Y.; Project administration, P.Y.; Resources, P.Y.; Software, Z.W.; Supervision, Z.W., W.T. and P.Y.; Validation, Z.W., S.S., Y.W., Z.Z., X.H. and P.Y.; Visualization, Z.W., S.S. and P.Y.; Writing—original draft, Z.W.; Writing—review & editing, Z.W., S.S. and P.Y. All authors have read and agreed to the published version of the manuscript.

**Funding:** P.Y. was supported by the scientific research starting funding of Shandong University (No. 1180509300002).

**Institutional Review Board Statement:** Not applicable.

**Informed Consent Statement:** Not applicable.

**Data Availability Statement:** All data are available on reasonable request to the corresponding author. Most of the data is sourced from publicly available databases.

**Acknowledgments:** We appreciate the experimental materials and theoretical guidance provided by Wei Zhang of Marine College, Shandong University, Weihai. Shenghai Shen would like to personally thank Fangyuan Zhang from Minjiang University for her support of his research work.

**Conflicts of Interest:** The authors declare no conflict of interest.

## References

1. Ahuja, I.; de Vos, R.C.H.; Bones, A.M.; Hall, R.D. Plant Molecular Stress Responses Face Climate Change. *Trends Plant Sci.* **2010**, *15*, 664–674. [[CrossRef](#)] [[PubMed](#)]
2. Miryeganeh, M. Plants' Epigenetic Mechanisms and Abiotic Stress. *Genes* **2021**, *12*, 1106. [[CrossRef](#)] [[PubMed](#)]
3. Rehaman, A.; Mishra, A.K.; Ferdose, A.; Per, T.S.; Hanief, M.; Jan, A.T.; Asgher, M. Melatonin in Plant Defense against Abiotic Stress. *Forests* **2021**, *12*, 1404. [[CrossRef](#)]
4. Naeem, M.; Shahzad, K.; Saqib, S.; Shahzad, A.; Nasrullah; Younas, M.; Afridi, M.I. The *Solanum Melongena* COP1LIKE Manipulates Fruit Ripening and Flowering Time in Tomato (*Solanum lycopersicum*). *Plant Growth Regul.* **2022**, *96*, 369–382. [[CrossRef](#)]
5. Han, G.; Qiao, Z.; Li, Y.; Yang, Z.; Wang, C.; Zhang, Y.; Liu, L.; Wang, B. RING Zinc Finger Proteins in Plant Abiotic Stress Tolerance. *Front. Plant Sci.* **2022**, *13*, 877011. [[CrossRef](#)]
6. Ayaz, A.; Huang, H.; Zheng, M.; Zaman, W.; Li, D.; Saqib, S.; Zhao, H.; Lü, S. Molecular Cloning and Functional Analysis of GmLACS2-3 Reveals Its Involvement in Cutin and Suberin Biosynthesis along with Abiotic Stress Tolerance. *Int. J. Mol. Sci.* **2021**, *22*, 9175. [[CrossRef](#)]
7. Rathour, M.; Shumayla; Alok, A.; Upadhyay, S.K. Investigation of Roles of TaTALE Genes during Development and Stress Response in Bread Wheat. *Plants* **2022**, *11*, 587. [[CrossRef](#)]

8. Bollier, N.; Gonzalez, N.; Chevalier, C.; Hernould, M. Zinc Finger-Homeodomain and Mini Zinc Finger Proteins Are Key Players in Plant Growth and Responses to Environmental Stresses. *J. Exp. Bot.* **2022**, *73*, 4662–4673. [[CrossRef](#)]
9. Han, G.; Li, Y.; Qiao, Z.; Wang, C.; Zhao, Y.; Guo, J.; Chen, M.; Wang, B. Advances in the Regulation of Epidermal Cell Development by C2H2 Zinc Finger Proteins in Plants. *Front. Plant Sci.* **2021**, *12*, 754512. [[CrossRef](#)]
10. Wang, K.; Ding, Y.; Cai, C.; Chen, Z.; Zhu, C. The Role of C2H2 Zinc Finger Proteins in Plant Responses to Abiotic Stresses. *Physiol. Plant.* **2019**, *165*, 690–700. [[CrossRef](#)]
11. Han, G.; Lu, C.; Guo, J.; Qiao, Z.; Sui, N.; Qiu, N.; Wang, B. C2H2 Zinc Finger Proteins: Master Regulators of Abiotic Stress Responses in Plants. *Front. Plant Sci.* **2020**, *11*, 115. [[CrossRef](#)]
12. Jiao, Z.; Wang, L.; Du, H.; Wang, Y.; Wang, W.; Liu, J.; Huang, J.; Huang, W.; Ge, L. Genome-Wide Study of C2H2 Zinc Finger Gene Family in *Medicago Truncatula*. *BMC Plant Biol.* **2020**, *20*, 401. [[CrossRef](#)] [[PubMed](#)]
13. Dutta, S.K.; Nimmakayala, P.; Reddy, U.K. Genome-Wide Identification, Characterisation, and Expression of C3HC4-Type RING Finger Gene Family in *Capsicum annuum* L. *J. Hort. Sci. Biotechnol.* **2022**, *97*, 603–614. [[CrossRef](#)]
14. Kim, D.H.; Yamaguchi, S.; Lim, S.; Oh, E.; Park, J.; Hanada, A.; Kamiya, Y.; Choi, G. SOMNUS, a CCCH-Type Zinc Finger Protein in Arabidopsis, Negatively Regulates Light-Dependent Seed Germination Downstream of PIL5. *Plant Cell* **2008**, *20*, 1260. [[CrossRef](#)] [[PubMed](#)]
15. Xu, D.-Q.; Huang, J.; Guo, S.-Q.; Yang, X.; Bao, Y.-M.; Tang, H.-J.; Zhang, H.-S. Overexpression of a TFIIIA-Type Zinc Finger Protein Gene ZFP252 Enhances Drought and Salt Tolerance in Rice (*Oryza sativa* L.). *FEBS Lett.* **2008**, *582*, 1037–1043. [[CrossRef](#)] [[PubMed](#)]
16. Cui, H.; Chen, J.; Liu, M.; Zhang, H.; Zhang, S.; Liu, D.; Chen, S. Genome-Wide Analysis of C2H2 Zinc Finger Gene Family and Its Response to Cold and Drought Stress in Sorghum [*Sorghum bicolor* (L.) Moench]. *Int. J. Mol. Sci.* **2022**, *23*, 5571. [[CrossRef](#)]
17. Tang, L.; Cai, H.; Ji, W.; Luo, X.; Wang, Z.; Wu, J.; Wang, X.; Cui, L.; Wang, Y.; Zhu, Y.; et al. Overexpression of GsZFP1 Enhances Salt and Drought Tolerance in Transgenic Alfalfa (*Medicago sativa* L.). *Plant Physiol. Biochem.* **2013**, *71*, 22–30. [[CrossRef](#)]
18. Aceituno-Valenzuela, U.; Micol-Ponce, R.; Ponce, M.R. Genome-Wide Analysis of CCHC-Type Zinc Finger (ZCCHC) Proteins in Yeast, Arabidopsis, and Humans. *Cell. Mol. Life Sci.* **2020**, *77*, 3991–4014. [[CrossRef](#)]
19. Wu, S.; Tong, X.; Li, C.; Lu, K.; Tan, D.; Hu, H.; Liu, H.; Dai, F. Genome-Wide Identification and Expression Profiling of the C2H2-Typ Zinc Finger Protein Genes in the Silkworm *Bombyx Mori*. *PeerJ* **2019**, *7*, e7222. [[CrossRef](#)]
20. Zhao, T.; Wu, T.; Zhang, J.; Wang, Z.; Pei, T.; Yang, H.; Li, J.; Xu, X. Genome-Wide Analyses of the Genetic Screening of C2H2-Type Zinc Finger Transcription Factors and Abiotic and Biotic Stress Responses in Tomato (*Solanum lycopersicum*) Based on RNA-Seq Data. *Front. Genet.* **2020**, *11*, 540. [[CrossRef](#)]
21. Ding, Q.; Zhao, H.; Zhu, P.; Jiang, X.; Nie, F.; Li, G. Genome-Wide Identification and Expression Analyses of C2H2 Zinc Finger Transcription Factors in *Pleurotus Ostreatus*. *PeerJ* **2022**, *10*, e12654. [[CrossRef](#)] [[PubMed](#)]
22. Chen, Y.; Wang, G.; Pan, J.; Wen, H.; Du, H.; Sun, J.; Zhang, K.; Lv, D.; He, H.; Cai, R.; et al. Comprehensive Genomic Analysis and Expression Profiling of the C2H2 Zinc Finger Protein Family under Abiotic Stresses in Cucumber (*Cucumis sativus* L.). *Genes* **2020**, *11*, 171. [[CrossRef](#)] [[PubMed](#)]
23. Brouns, F.R.; van Rooy, G.; Shewry, P.; Rustgi, S.; Jonkers, D. Adverse Reactions to Wheat or Wheat Components. *Compr. Rev. Food Sci. Food Saf.* **2019**, *18*, 1437–1452. [[CrossRef](#)] [[PubMed](#)]
24. Shewry, P.R. Wheat. *J. Exp. Bot.* **2009**, *60*, 1537–1553. [[CrossRef](#)] [[PubMed](#)]
25. Sallam, A.; Alqudah, A.M.; Dawood, M.F.A.; Baenziger, P.S.; Börner, A. Drought Stress Tolerance in Wheat and Barley: Advances in Physiology, Breeding and Genetics Research. *Int. J. Mol. Sci.* **2019**, *20*, 3137. [[CrossRef](#)]
26. Sun, A.; Li, Y.; He, Y.; Zou, X.; Chen, F.; Ji, R.; You, C.; Yu, K.; Li, Y.; Xiao, W.; et al. Comprehensive Genome-Wide Identification, Characterization, and Expression Analysis of CCHC-Type Zinc Finger Gene Family in Wheat (*Triticum aestivum* L.). *Front. Plant Sci.* **2022**, *13*, 892105. [[CrossRef](#)]
27. Faraji, S.; Rasouli, S.H.; Kazemitabar, S.K. Genome-Wide Exploration of C2H2 Zinc Finger Family in Durum Wheat (*Triticum Turgidum* Ssp. Durum): Insights into the Roles in Biological Processes Especially Stress Response. *Biometals* **2018**, *31*, 1019–1042. [[CrossRef](#)]
28. Ma, R.; Chen, J.; Huang, B.; Huang, Z.; Zhang, Z. The BBX Gene Family in Moso Bamboo (*Phyllostachys edulis*): Identification, Characterization and Expression Profiles. *BMC Genom.* **2021**, *22*, 533. [[CrossRef](#)]
29. He, P.; Yang, Y.; Wang, Z.; Zhao, P.; Yuan, Y.; Zhang, L.; Ma, Y.; Pang, C.; Yu, J.; Xiao, G. Comprehensive Analyses of ZFP Gene Family and Characterization of Expression Profiles during Plant Hormone Response in Cotton. *BMC Plant Biol.* **2019**, *19*, 329. [[CrossRef](#)]
30. Kesawat, M.S.; Kherawat, B.S.; Singh, A.; Dey, P.; Routray, S.; Mohapatra, C.; Saha, D.; Ram, C.; Siddique, K.H.M.; Kumar, A.; et al. Genome-Wide Analysis and Characterization of the Proline-Rich Extensin-like Receptor Kinases (PERKs) Gene Family Reveals Their Role in Different Developmental Stages and Stress Conditions in Wheat (*Triticum aestivum* L.). *Plants* **2022**, *11*, 496. [[CrossRef](#)]
31. Iuchi, S. Three Classes of C2H2 Zinc Finger Proteins. *CMLS Cell. Mol. Life Sci.* **2001**, *58*, 625–635. [[CrossRef](#)] [[PubMed](#)]
32. Winicov, I. Alfin1 Transcription Factor Overexpression Enhances Plant Root Growth under Normal and Saline Conditions and Improves Salt Tolerance in Alfalfa. *Planta* **2000**, *210*, 416–422. [[CrossRef](#)] [[PubMed](#)]
33. Alam, I.; Batool, K.; Cui, D.-L.; Yang, Y.-Q.; Lu, Y.-H. Comprehensive Genomic Survey, Structural Classification and Expression Analysis of C2H2 Zinc Finger Protein Gene Family in *Brassica rapa* L. *PLoS ONE* **2019**, *14*, e0216071. [[CrossRef](#)]

34. Smith, A.E.F.; Farzaneh, F.; Ford, K.G. Single Zinc-Finger Extension: Enhancing Transcriptional Activity and Specificity of Three-Zinc-Finger Proteins. *Biol. Chem.* **2005**, *386*, 95–99. [[CrossRef](#)] [[PubMed](#)]
35. Hiratsuka, K.; Chua, N.-H. Light Regulated Transcription in Higher Plants. *J. Plant Res.* **1997**, *110*, 131–139. [[CrossRef](#)]
36. Manjunath, S.; Sachs, M.M. Molecular Characterization and Promoter Analysis of the Maize Cytosolic Glyceraldehyde 3-Phosphate Dehydrogenase Gene Family and Its Expression during Anoxia. *Plant Mol. Biol.* **1997**, *33*, 97–112. [[CrossRef](#)]
37. Thomashow, M.F. Plant Cold Acclimation: Freezing Tolerance Genes and Regulatory Mechanisms. *Annu. Rev. Plant Physiol. Plant Mol. Biol.* **1999**, *50*, 571–599. [[CrossRef](#)]
38. Geffers, R.; Sell, S.; Cerff, R.; Hehl, R. The TATA Box and a Myb Binding Site Are Essential for Anaerobic Expression of a Maize GapC4 Minimal Promoter in Tobacco. *Biochim. Biophys. Acta (BBA)-Gene Struct. Expr.* **2001**, *1521*, 120–125. [[CrossRef](#)]
39. Xu, R. Genome-Wide Analysis and Identification of Stress-Responsive Genes of the CCCH Zinc Finger Family in *Solanum lycopersicum*. *Mol. Genet. Genom.* **2014**, *289*, 965–979. [[CrossRef](#)]
40. Ming, N.; Ma, N.; Jiao, B.; Lv, W.; Meng, Q. Genome Wide Identification of C2H2-Type Zinc Finger Proteins of Tomato and Expression Analysis Under Different Abiotic Stresses. *Plant Mol. Biol. Rep.* **2020**, *38*, 75–94. [[CrossRef](#)]
41. Guk, J.-Y.; Jang, M.-J.; Kim, S. Identification of Novel PHD-Finger Genes in Pepper by Genomic Re-Annotation and Comparative Analyses. *BMC Plant Biol.* **2022**, *22*, 206. [[CrossRef](#)] [[PubMed](#)]
42. Pi, B.; He, X.; Ruan, Y.; Jang, J.-C.; Huang, Y. Genome-Wide Analysis and Stress-Responsive Expression of CCCH Zinc Finger Family Genes in Brassica Rapa. *BMC Plant Biol.* **2018**, *18*, 373. [[CrossRef](#)] [[PubMed](#)]
43. Lu, P.; Magwanga, R.O.; Guo, X.; Kirungu, J.N.; Lu, H.; Cai, X.; Zhou, Z.; Wei, Y.; Wang, X.; Zhang, Z.; et al. Genome-Wide Analysis of Multidrug and Toxic Compound Extrusion (MATE) Family in *Gossypium Raimondii* and *Gossypium Arboreum* and Its Expression Analysis Under Salt, Cadmium, and Drought Stress. *G3-Genes Genomes Genet.* **2018**, *8*, 2483–2500. [[CrossRef](#)] [[PubMed](#)]
44. Liu, Z.; Xin, M.; Qin, J.; Peng, H.; Ni, Z.; Yao, Y.; Sun, Q. Temporal Transcriptome Profiling Reveals Expression Partitioning of Homeologous Genes Contributing to Heat and Drought Acclimation in Wheat (*Triticum aestivum* L.). *BMC Plant Biol.* **2015**, *15*, 152. [[CrossRef](#)] [[PubMed](#)]
45. Liu, H.; Yang, Y.; Zhang, L. Zinc Finger-Homeodomain Transcriptional Factors (ZF-HDs) in Wheat (*Triticum aestivum* L.): Identification, Evolution, Expression Analysis and Response to Abiotic Stresses. *Plants* **2021**, *10*, 593. [[CrossRef](#)] [[PubMed](#)]
46. Han, G.; Qiao, Z.; Li, Y.; Wang, C.; Wang, B. The Roles of CCCH Zinc-Finger Proteins in Plant Abiotic Stress Tolerance. *Int. J. Mol. Sci.* **2021**, *22*, 8327. [[CrossRef](#)]
47. Gao, Y.; Liu, H.; Wang, Y.; Li, F.; Xiang, Y. Genome-Wide Identification of PHD-Finger Genes and Expression Pattern Analysis under Various Treatments in Moso Bamboo (*Phyllostachys edulis*). *Plant Physiol. Biochem.* **2018**, *123*, 378–391. [[CrossRef](#)]
48. Peng, X.; Zhao, Y.; Cao, J.; Zhang, W.; Jiang, H.; Li, X.; Ma, Q.; Zhu, S.; Cheng, B. CCCH-Type Zinc Finger Family in Maize: Genome-Wide Identification, Classification and Expression Profiling under Abscisic Acid and Drought Treatments. *PLoS ONE* **2012**, *7*, e40120. [[CrossRef](#)]
49. Liang, Y.; Xiong, Z.; Zheng, J.; Xu, D.; Zhu, Z.; Xiang, J.; Gan, J.; Raboanatahiry, N.; Yin, Y.; Li, M. Genome-Wide Identification, Structural Analysis and New Insights into Late Embryogenesis Abundant (LEA) Gene Family Formation Pattern in *Brassica napus*. *Sci. Rep.* **2016**, *6*, 24265. [[CrossRef](#)]
50. Shumayla; Mendu, V.; Singh, K.; Upadhyay, S.K. Insight into the Roles of Proline-Rich Extensin-like Receptor Protein Kinases of Bread Wheat (*Triticum aestivum* L.). *Life* **2022**, *12*, 941. [[CrossRef](#)]
51. Shumayla; Madhu; Singh, K.; Upadhyay, S.K. LysM Domain-Containing Proteins Modulate Stress Response and Signalling in *Triticum aestivum* L. *Environ. Exp. Bot.* **2021**, *189*, 104558. [[CrossRef](#)]
52. Park, H.-Y.; Lee, K.C.; Jang, Y.H.; Kim, S.-K.; Thu, M.P.; Lee, J.H.; Kim, J.-K. The Arabidopsis Splicing Factors, AtU2AF65, AtU2AF35, and AtSF1 Shuttle between Nuclei and Cytoplasm. *Plant Cell Rep.* **2017**, *36*, 1113–1123. [[CrossRef](#)] [[PubMed](#)]
53. Wang, B.B.; Brendel, V. Molecular Characterization and Phylogeny of U2AF(35) Homologs in Plants. *Plant Physiol.* **2006**, *140*, 624–636. [[CrossRef](#)] [[PubMed](#)]
54. Agarwal, P.; Arora, R.; Ray, S.; Singh, A.K.; Singh, V.P.; Takatsuji, H.; Kapoor, S.; Tyagi, A.K. Genome-Wide Identification of C2H2 Zinc-Finger Gene Family in Rice and Their Phylogeny and Expression Analysis. *Plant Mol. Biol.* **2007**, *65*, 467–485. [[CrossRef](#)]
55. Zhang, S.; Liu, J.; Zhong, G.; Wang, B. Genome-Wide Identification and Expression Patterns of the C2H2-Zinc Finger Gene Family Related to Stress Responses and Catechins Accumulation in *Camellia sinensis* [L.] O. Kuntze. *Int. J. Mol. Sci.* **2021**, *22*, 4197. [[CrossRef](#)]
56. Wang, D.; Guo, Y.; Wu, C.; Yang, G.; Li, Y.; Zheng, C. Genome-Wide Analysis of CCCH Zinc Finger Family in Arabidopsis and Rice. *BMC Genom.* **2008**, *9*, 44. [[CrossRef](#)]
57. Wan, Y.; Wang, Z.; Xia, J.; Shen, S.; Guan, M.; Zhu, M.; Qiao, C.; Sun, F.; Liang, Y.; Li, J.; et al. Genome-Wide Analysis of Phosphorus Transporter Genes in Brassica and Their Roles in Heavy Metal Stress Tolerance. *Int. J. Mol. Sci.* **2020**, *21*, 2209. [[CrossRef](#)]
58. Taylor, J.S.; Raes, J. Duplication and Divergence: The Evolution of New Genes and Old Ideas. *Annu. Rev. Genet.* **2004**, *38*, 615–643. [[CrossRef](#)]
59. Hao, Y.; Hao, M.; Cui, Y.; Kong, L.; Wang, H. Genome-Wide Survey of the Dehydrin Genes in Bread Wheat (*Triticum aestivum* L.) and Its Relatives: Identification, Evolution and Expression Profiling under Various Abiotic Stresses. *BMC Genom.* **2022**, *23*, 73. [[CrossRef](#)]

60. Dong, L.; Lu, Y.; Liu, S. Genome-Wide Member Identification, Phylogeny and Expression Analysis of PEBP Gene Family in Wheat and Its Progenitors. *PeerJ* **2020**, *8*, e10483. [[CrossRef](#)]
61. Jiang, Y.; Liu, L.; Pan, Z.; Zhao, M.; Zhu, L.; Han, Y.; Li, L.; Wang, Y.; Wang, K.; Liu, S.; et al. Genome-Wide Analysis of the C2H2 Zinc Finger Protein Gene Family and Its Response to Salt Stress in Ginseng, *Panax Ginseng Meyer*. *Sci. Rep.* **2022**, *12*, 10165. [[CrossRef](#)] [[PubMed](#)]
62. Malik, W.A.; Wang, X.; Wang, X.; Shu, N.; Cui, R.; Chen, X.; Wang, D.; Lu, X.; Yin, Z.; Wang, J.; et al. Genome-Wide Expression Analysis Suggests Glutaredoxin Genes Response to Various Stresses in Cotton. *Int. J. Biol. Macromol.* **2020**, *153*, 470–491. [[CrossRef](#)] [[PubMed](#)]
63. Kumar, A.; Sharma, S.; Chunduri, V.; Kaur, A.; Kaur, S.; Malhotra, N.; Kumar, A.; Kapoor, P.; Kumari, A.; Kaur, J.; et al. Genome-Wide Identification and Characterization of Heat Shock Protein Family Reveals Role in Development and Stress Conditions in *Triticum aestivum* L. *Sci. Rep.* **2020**, *10*, 7858. [[CrossRef](#)] [[PubMed](#)]
64. Fedorova, L.; Fedorov, A. Introns in Gene Evolution. *Genetica* **2003**, *118*, 123–131. [[CrossRef](#)] [[PubMed](#)]
65. Deshmukh, R.K.; Sonah, H.; Singh, N.K. Intron Gain, a Dominant Evolutionary Process Supporting High Levels of Gene Expression in Rice. *J. Plant Biochem. Biotechnol.* **2016**, *25*, 142–146. [[CrossRef](#)]
66. Yu, P.; Shinde, H.; Dudhate, A.; Tsugama, D.; Gupta, S.K.; Liu, S.; Takano, T. Genome-Wide Investigation of SQUAMOSA Promoter Binding Protein-like Transcription Factor Family in Pearl Millet (*Pennisetum glaucum* (L.) R. Br.). *Plant Gene* **2021**, *27*, 100313. [[CrossRef](#)]
67. Singh, S.; Kudapa, H.; Garg, V.; Varshney, R.K. Comprehensive Analysis and Identification of Drought-Responsive Candidate NAC Genes in Three Semi-Arid Tropics (SAT) Legume Crops. *BMC Genom.* **2021**, *22*, 289. [[CrossRef](#)]
68. Li, K.; Xing, C.; Yao, Z.; Huang, X. PbrMYB21, a Novel MYB Protein of *Pyrus Betulaefolia*, Functions in Drought Tolerance and Modulates Polyamine Levels by Regulating Arginine Decarboxylase Gene. *Plant Biotechnol. J.* **2017**, *15*, 1186–1203. [[CrossRef](#)]
69. Tyagi, A.K.; Gaur, T. Light Regulation of Nuclear Photosynthetic Genes in Higher Plants. *Crit. Rev. Plant Sci.* **2003**, *22*, 417–452. [[CrossRef](#)]
70. Fankhauser, C.; Chory, J. Light Control of Plant Development. *Annu. Rev. Cell Dev. Biol.* **1997**, *13*, 203–229. [[CrossRef](#)]
71. Baldoni, E.; Genga, A.; Cominelli, E. Plant MYB Transcription Factors: Their Role in Drought Response Mechanisms. *Int. J. Mol. Sci.* **2015**, *16*, 15811–15851. [[CrossRef](#)] [[PubMed](#)]
72. Han, Y.; Hou, Z.; He, Q.; Zhang, X.; Yan, K.; Han, R.; Liang, Z. Genome-Wide Characterization and Expression Analysis of BZIP Gene Family Under Abiotic Stress in *Glycyrrhiza uralensis*. *Front. Genet.* **2021**, *12*, 754237. [[CrossRef](#)] [[PubMed](#)]
73. Baillo, E.H.; Hanif, M.S.; Guo, Y.; Zhang, Z.; Xu, P.; Algam, S.A. Genome-Wide Identification of WRKY Transcription Factor Family Members in Sorghum (*Sorghum bicolor* (L.) Moench). *PLoS ONE* **2020**, *15*, e0236651. [[CrossRef](#)] [[PubMed](#)]
74. Ashburner, M.; Ball, C.A.; Blake, J.A.; Botstein, D.; Butler, H.; Cherry, J.M.; Davis, A.P.; Dolinski, K.; Dwight, S.S.; Eppig, J.T.; et al. Gene Ontology: Tool for the Unification of Biology. The Gene Ontology Consortium. *Nat. Genet.* **2000**, *25*, 25–29. [[CrossRef](#)] [[PubMed](#)]
75. Kolodziej, M.C.; Singla, J.; Sanchez-Martin, J.; Zbinden, H.; Simkova, H.; Karafiatova, M.; Dolezel, J.; Gronnier, J.; Poretti, M.; Glauser, G.; et al. A Membrane-Bound Ankyrin Repeat Protein Confers Race-Specific Leaf Rust Disease Resistance in Wheat. *Nat. Commun.* **2021**, *12*, 956. [[CrossRef](#)]
76. Yu, S.; Liao, F.; Wang, F.; Wen, W.; Li, J.; Mei, H.; Luo, L. Identification of Rice Transcription Factors Associated with Drought Tolerance Using the Ecotilling Method. *PLoS ONE* **2012**, *7*, e30765. [[CrossRef](#)]
77. Daetwyler, H.D.; Pong-Wong, R.; Villanueva, B.; Woolliams, J.A. The Impact of Genetic Architecture on Genome-Wide Evaluation Methods. *Genetics* **2010**, *185*, 1021–1031. [[CrossRef](#)]
78. Tsukada, Y.; Fang, J.; Erdjument-Bromage, H.; Warren, M.E.; Borchers, C.H.; Tempst, P.; Zhang, Y. Histone Demethylation by a Family of JmjC Domain-Containing Proteins. *Nature* **2006**, *439*, 811–816. [[CrossRef](#)]
79. Yaschenko, A.E.; Fenech, M.; Mazzoni-Putman, S.; Alonso, J.M.; Stepanova, A.N. Deciphering the Molecular Basis of Tissue-Specific Gene Expression in Plants: Can Synthetic Biology Help? *Curr. Opin. Plant Biol.* **2022**, *68*, 102241. [[CrossRef](#)]
80. Duan, H.; Zhu, Y.; Li, J.; Ding, W.; Wang, H.; Jiang, L.; Zhou, Y. Effects of Drought Stress on Growth and Development of Wheat Seedlings. *Int. J. Agric. Biol.* **2017**, *19*, 1119–1124. [[CrossRef](#)]
81. Qin, F.; Sakuma, Y.; Tran, L.-S.P.; Maruyama, K.; Kidokoro, S.; Fujita, Y.; Fujita, M.; Umezawa, T.; Sawano, Y.; Miyazono, K.; et al. Arabidopsis DREB2A-Interacting Proteins Function as RING E3 Ligases and Negatively Regulate Plant Drought Stress-Responsive Gene Expression. *Plant Cell* **2008**, *20*, 1693–1707. [[CrossRef](#)] [[PubMed](#)]
82. Wang, P.; Yang, C.; Chen, H.; Luo, L.; Leng, Q.; Li, S.; Han, Z.; Li, X.; Song, C.; Zhang, X.; et al. Exploring Transcription Factors Reveals Crucial Members and Regulatory Networks Involved in Different Abiotic Stresses in *Brassica napus* L. *BMC Plant Biol.* **2018**, *18*, 202. [[CrossRef](#)] [[PubMed](#)]
83. Zhang, C.; Yang, Q.; Zhang, X.; Zhang, X.; Yu, T.; Wu, Y.; Fang, Y.; Xue, D. Genome-Wide Identification of the HMA Gene Family and Expression Analysis under Cd Stress in Barley. *Plants* **2021**, *10*, 1849. [[CrossRef](#)] [[PubMed](#)]
84. Yang, L.; Cao, H.; Zhang, X.; Gui, L.; Chen, Q.; Qian, G.; Xiao, J.; Li, Z. Genome-Wide Identification and Expression Analysis of Tomato ADK Gene Family during Development and Stress. *Int. J. Mol. Sci.* **2021**, *22*, 7708. [[CrossRef](#)] [[PubMed](#)]
85. Price, M.N.; Dehal, P.S.; Arkin, A.P. FastTree: Computing Large Minimum Evolution Trees with Profiles Instead of a Distance Matrix. *Mol. Biol. Evol.* **2009**, *26*, 1641–1650. [[CrossRef](#)]



86. Price, M.N.; Dehal, P.S.; Arkin, A.P. FastTree 2-Approximately Maximum-Likelihood Trees for Large Alignments. *PLoS ONE* **2010**, *5*, e9490. [[CrossRef](#)]
87. Wang, Y.; Tang, H.; Debarry, J.D.; Tan, X.; Li, J.; Wang, X.; Lee, T.; Jin, H.; Marler, B.; Guo, H.; et al. MCScanX: A Toolkit for Detection and Evolutionary Analysis of Gene Synteny and Collinearity. *Nucleic Acids Res.* **2012**, *40*, e49. [[CrossRef](#)]
88. Sharma, A.; Sharma, H.; Rajput, R.; Pandey, A.; Upadhyay, S.K. Molecular Characterization Revealed the Role of Thaumatin-Like Proteins of Bread Wheat in Stress Response. *Front. Plant Sci.* **2022**, *12*, 807448. [[CrossRef](#)]
89. Gaut, B.S.; Morton, B.R.; McCaig, B.C.; Clegg, M.T. Substitution Rate Comparisons between Grasses and Palms: Synonymous Rate Differences at the Nuclear Gene *Adh* Parallel Rate Differences at the Plastid Gene *RbcL*. *Proc. Natl. Acad. Sci. USA* **1996**, *93*, 10274–10279. [[CrossRef](#)]
90. Letunic, I.; Khedkar, S.; Bork, P. SMART: Recent Updates, New Developments and Status in 2020. *Nucleic Acids Res.* **2021**, *49*, D458–D460. [[CrossRef](#)]
91. Shannon, P.; Markiel, A.; Ozier, O.; Baliga, N.S.; Wang, J.T.; Ramage, D.; Amin, N.; Schwikowski, B.; Ideker, T. Cytoscape: A Software Environment for Integrated Models of Biomolecular Interaction Networks. *Genome Res.* **2003**, *13*, 2498–2504. [[CrossRef](#)] [[PubMed](#)]
92. Ma, S.; Wang, M.; Wu, J.; Guo, W.; Chen, Y.; Li, G.; Wang, Y.; Shi, W.; Xia, G.; Fu, D.; et al. WheatOmics: A Platform Combining Multiple Omics Data to Accelerate Functional Genomics Studies in Wheat. *Mol. Plant* **2021**, *14*, 1965–1968. [[CrossRef](#)] [[PubMed](#)]
93. Wang, Y.; Zhang, Y.; Fan, C.; Wei, Y.; Meng, J.; Li, Z.; Zhong, C. Genome-Wide Analysis of MYB Transcription Factors and Their Responses to Salt Stress in *Casuarina equisetifolia*. *BMC Plant Biol.* **2021**, *21*, 328. [[CrossRef](#)]
94. Livak, K.J.; Schmittgen, T.D. Analysis of Relative Gene Expression Data Using Real-Time Quantitative PCR and the 2<sup>-</sup>(Delta Delta C(T)) Method. *Methods* **2001**, *25*, 402–408. [[CrossRef](#)] [[PubMed](#)]